ANALYZING AND SIMULATING THE COHERENT CONTROL MODEL

Luuk Lubbers and Sean Stellingwerff

Supervisors: Prof. Dr. Jennifer Herek and Dr. Ir. Herman L. Offerhaus

Enschede, April 13, 2011

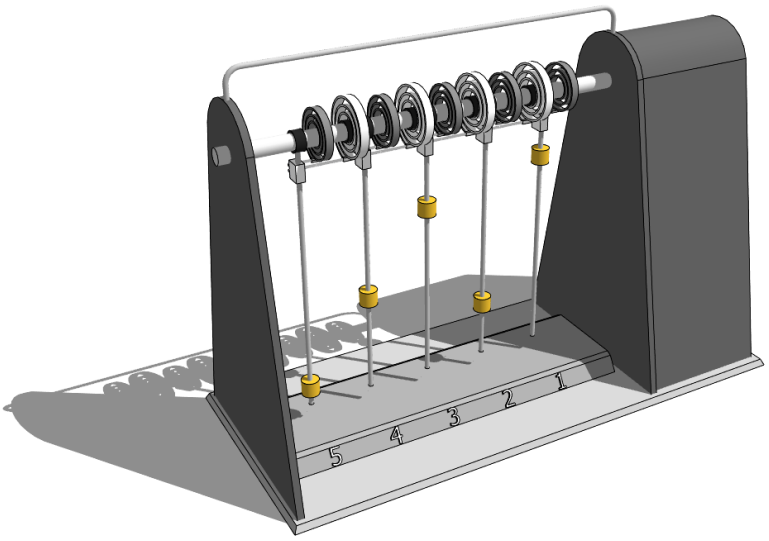

UNIVERSITY OF TWENTE.

Abstract

A theoretical description and a simulation model for a coherent control model was derived and was experimentally verified. First, a simplified version of the coherent control model, where no distinction is made between pendula lengths, masses and spring constants, was considered and the equations of motion for that particular system were derived. This theoretical description was then analyzed, after which it was expanded to include all relevant parameters in the system.

The theoretical description was then implemented in a simulation model and this simulation model was subjected to various tests to ensure that is was performing as expected. To that end, both the experimental set-up and the simulation model were driven with a continuous sinusoidal shaped drive signal, of which the driving frequency ω was iteratively increased from small to large values and the response of both systems was measured and compared. After verifying that the response of the simulation model adequately predicted the output of the experimental set-up, the lengths of various pendula were changed and the predicted response from the simulation model was compared to the response of the experimental set-up.

In the final part of the research, the link between CARS and the coherent control model was briefly discussed. The theory behind using a drive pulse instead of a continuous sinusoidal shaped drive signal was explained and the simulation model was subsequently subjected to a drive pulse to analyze its response. Lastly, the drive pulse was altered in the phase spectrum and the output of the simulation model was compared to the unaltered drive pulse response.

Contents

Chapter 1

Introduction

1.1 Coherent anti-Stokes Raman spectroscopy

Coherent anti-Stokes Raman spectroscopy, also known as CARS, is a spectroscopy method used to visualize specific bonds in a molecule. A narrow-band pulse[1] could theoretically be used to excite one particular bond in a molecule, the energy that is stored in that bond will quickly dissipate into other bonds in the same molecule, leading to a loss of detection signal. To reduce the loss of detection signal, a method called coherent control is often used. It works by shaping the pulse that is originally used to excite one specific bond to now excite all bonds in the molecule in such as way that the vibrations will (de)constructively interfere so that only the bond of interest will remaing vibrating.

1.2 Description of the demonstration model

In order to make the concept of coherent control comprehensible, a demonstration model - a system of five coupled pendula driven by a motor - has been built previously. The pendulum model is schematically drawn in figure 1.1. The set-up consists of five coupled pendula, each coupled to its neighbouring pendula if present and also to a central drive axle. This drive axle is controlled by a motor which can in turn be controlled by a computer. This way, the pendulum model can be driven using various drive pulses in order to demonstrate the effect of an unoptimized and an optimized pulse. Using motion sensors, the movement of each pendulum is sent back to the computer which can in turn process the data and make changes to the drive pulse, if necessary.

To illustrate how each pendulum is connected to the drive axle and to neighbouring pendula, a close-up of the schematic drawing has been made, see figure 1.2.

[1] This is a pulse with a selective range of frequencies

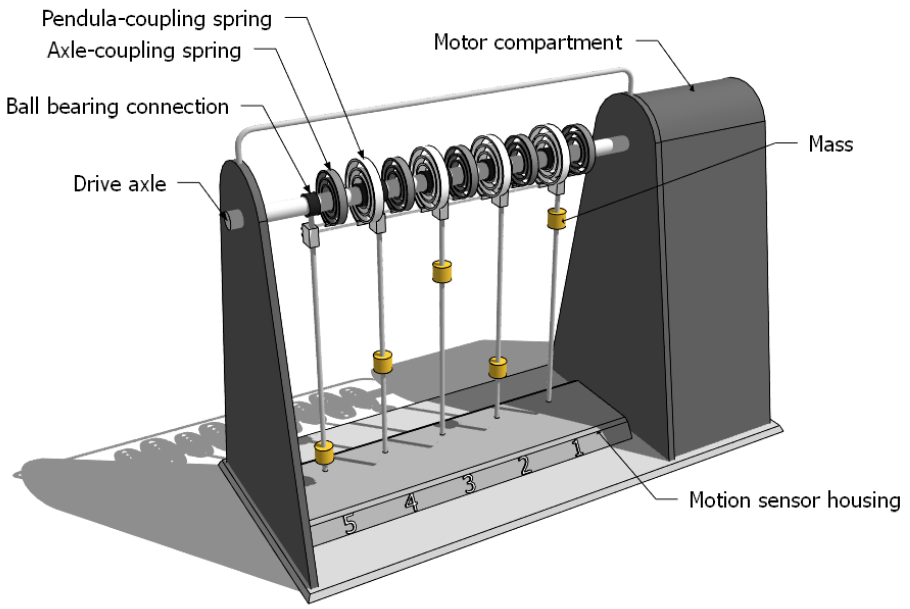

Figure 1.1: Schematic overview of the coherent control model

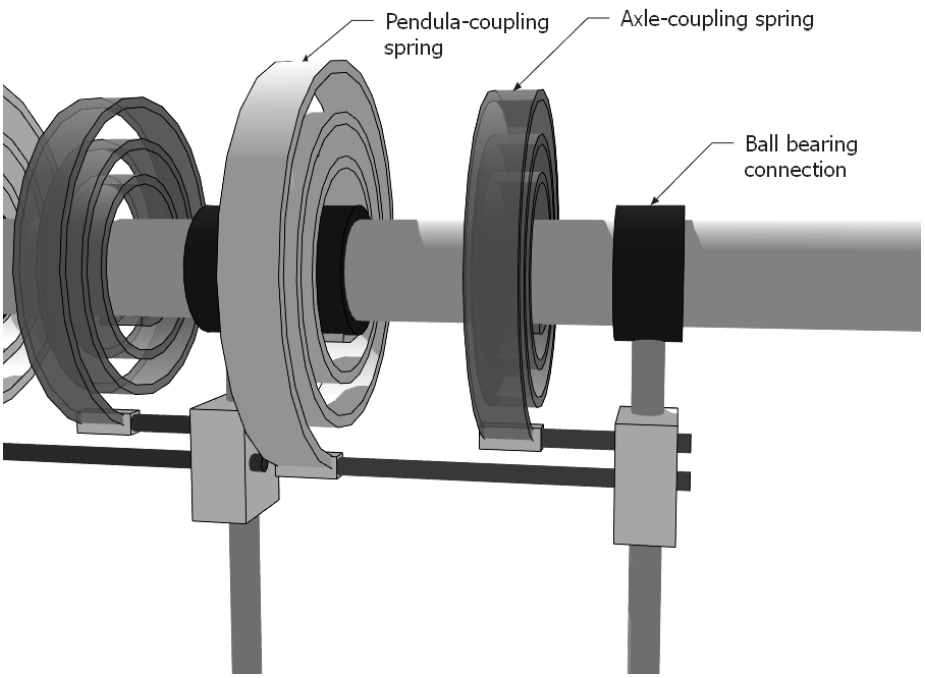

Figure 1.2: Schematic close-up of the connections between neighbouring pendula and the drive axle

If there were no springs to attach each of the pendula to the axle or to a neighbouring pendulum, the pendula would be able to swing freely, independent of the drive axle's motion. This is achieved by using ball bearings to connect each pendulum to the axle as indicated in the schematic close-up. This way, the pendula can only be indirectly driven by the drive axle through the axle-coupling springs and each pendulum will affect the motion of its neighbouring pendula through the pendulum-coupling springs.

1.3 Thesis outline

The goal of this thesis is to analyze this pendulum set-up and to describe it theoretically. In Chapter 2, a simplified version of the pendulum set-up will be used to derive a simple theoretical model, after which this model will be briefly analyzed. Then this simple model will be expanded to include all relevant parameters in the system. Using this extended theoretical description of the set-up, a simulation model will be constructed in Chapter 3. The validity of this model will then be discussed in Chapter 4 and a few predictions will be made using it. In Chapter 5, drive pulses as used in CARS will be sent into the simulation model and the response of the system will be analyzed in the case that the pulses are optimized and are unoptimized. Finally, the results of the report will be discussed and the conclusions will be presented at the end of the report.

Chapter 2

Theoretical description of the set-up

In this chapter, a theoretical model of the pendulum set-up will be derived. First, a simple version of the set-up will be used to build a simple simulation model. This model will be analyzed to verify that the output is as can be expected, after which the model will be expanded to include parameters such as damping and varying spring constants.

2.1 The basics, simple system, amplitude response

Now that a clear picture has been formed of the pendulum set-up, it can be theoretically described so that a simulation model can be built. It is wise to start with a simple model in order to be able to analyze the simulation step by step, and to make sure that it is performing as it should. For this, initially the lengths l of the different pendula as well as their masses m and the spring constants of each type of spring in the system are chosen to be the same. Damping will also not be considered initially.

As mentioned, each of the pendula will ultimately be indirectly driven by a motor. The motor will turn a drive axle which will have an angle of γ relative to the vertical. Through a coupling spring, with spring constant κ, that is connected to the drive axle and the pendulum itself, a force will be exerted on the pendulum. That force will be nonzero when the angle between the drive axle and the pendulum, which is defined to be $\theta_n - \gamma$, is nonzero, where θ_n is the angle of the nth pendulum relative to the vertical.

Additionally, each pendulum is connected by pendulum-coupling springs, with spring constant $\widetilde{\kappa}$, to its neighbouring pendula. That way each pendulum will affect and will be affected by its neighbouring pendula. However, because of the set-up, not all pendula have two neighbours, some only have one. See Figure 1.1 for a schematic drawing, illustrating this.

The kinetic energy T_1 and the potential energy U_1 of pendulum 1, which has only one neighbour, is given by

$$T_1 = \frac{1}{2}m(\dot{\theta_1}l)^2 = \frac{1}{2}ml^2\dot{\theta_1^2}$$

$$\begin{aligned} U_1 &= mgy + \frac{1}{2}\kappa(\theta_1 - \gamma)^2 + \frac{1}{2}\tilde{\kappa}(\theta_1 - \theta_2)^2 \\ &= -mglcos(\theta_1) + \frac{1}{2}\kappa(\theta_1 - \gamma)^2 + \frac{1}{2}\tilde{\kappa}(\theta_1 - \theta_2)^2 \end{aligned}$$

Where g is the gravitational acceleration and y is the vertical position of the mass[1].

For pendula that have two neighbouring pendula (namely pendula 2 through 4) the kinetic and potential energies are given by

$$T_n = \frac{1}{2}m(\dot{\theta_n}l)^2 = \frac{1}{2}ml^2\dot{\theta_n^2}$$

$$\begin{aligned} U_n &= mgy + \frac{1}{2}\kappa(\theta_n - \gamma)^2 + \frac{1}{2}\tilde{\kappa}(\theta_n - \theta_{n-1})^2 + \frac{1}{2}\tilde{\kappa}(\theta_n - \theta_{n+1})^2 \\ &= -mglcos(\theta_n) + \frac{1}{2}\kappa(\theta_n - \gamma)^2 + \frac{1}{2}\tilde{\kappa}(\theta_n - \theta_{n-1})^2 + \frac{1}{2}\tilde{\kappa}(\theta_n - \theta_{n+1})^2 \end{aligned}$$

where $n \in \{2, 3, 4\}$.

Finally, for pendulum 5, which like pendulum 1 only has one neighbouring pendulum, the kinetic and potential energies are given by

$$T_5 = \frac{1}{2}m(\dot{\theta_5}l)^2 = \frac{1}{2}ml^2\dot{\theta_5^2}$$

$$\begin{aligned} U_5 &= mgy + \frac{1}{2}\kappa(\theta_5 - \gamma)^2 + \frac{1}{2}\tilde{\kappa}(\theta_5 - \theta_4)^2 \\ &= -mglcos(\theta_5) + \frac{1}{2}\kappa(\theta_5 - \gamma)^2 + \frac{1}{2}\tilde{\kappa}(\theta_5 - \theta_4)^2 \end{aligned}$$

Going one step further, the Lagrangians $L_n \equiv T_n - U_n$ for $n \in \{1, 2, 3, 4, 5\}$ are then given by

$$\begin{aligned} L_1 &= \frac{1}{2}ml^2\dot{\theta_1^2} + mglcos(\theta_1) - \frac{1}{2}\kappa(\theta_1 - \gamma)^2 - \frac{1}{2}\tilde{\kappa}(\theta_1 - \theta_2)^2 \\ L_2 &= \frac{1}{2}ml^2\dot{\theta_2^2} + mglcos(\theta_2) - \frac{1}{2}\kappa(\theta_2 - \gamma)^2 - \frac{1}{2}\tilde{\kappa}(\theta_2 - \theta_1)^2 - \frac{1}{2}\tilde{\kappa}(\theta_2 - \theta_3)^2 \\ L_3 &= \frac{1}{2}ml^2\dot{\theta_3^2} + mglcos(\theta_3) - \frac{1}{2}\kappa(\theta_3 - \gamma)^2 - \frac{1}{2}\tilde{\kappa}(\theta_3 - \theta_2)^2 - \frac{1}{2}\tilde{\kappa}(\theta_3 - \theta_4)^2 \\ L_4 &= \frac{1}{2}ml^2\dot{\theta_4^2} + mglcos(\theta_4) - \frac{1}{2}\kappa(\theta_4 - \gamma)^2 - \frac{1}{2}\tilde{\kappa}(\theta_4 - \theta_3)^2 - \frac{1}{2}\tilde{\kappa}(\theta_4 - \theta_5)^2 \\ L_5 &= \frac{1}{2}ml^2\dot{\theta_5^2} + mglcos(\theta_5) - \frac{1}{2}\kappa(\theta_5 - \gamma)^2 - \frac{1}{2}\tilde{\kappa}(\theta_5 - \theta_4)^2 \end{aligned}$$

[1] Here $y = 0$ at the center of the drive axle and is defined to be negative downward.

The equations of motions for this system now follow from Lagrange's equation[2],

$$\frac{\partial}{\partial t}\left(\frac{\partial L}{\partial \dot{\theta}_n}\right) - \frac{\partial L}{\partial \theta_n} = 0$$

Carrying out the differentiation for each Langrangian gives a set of five coupled non-linear second order differential equations

$$\left.\begin{array}{rcl}
\ddot{\theta}_1 + \frac{g}{l} sin(\theta_1) + a(\theta_1 - \gamma) + b(\theta_1 - \theta_2) & = & 0 \\
\ddot{\theta}_2 + \frac{g}{l} sin(\theta_2) + a(\theta_2 - \gamma) + b(\theta_2 - \theta_1) + b(\theta_2 - \theta_3) & = & 0 \\
\ddot{\theta}_3 + \frac{g}{l} sin(\theta_3) + a(\theta_3 - \gamma) + b(\theta_3 - \theta_2) + b(\theta_3 - \theta_4) & = & 0 \\
\ddot{\theta}_4 + \frac{g}{l} sin(\theta_4) + a(\theta_4 - \gamma) + b(\theta_4 - \theta_3) + b(\theta_4 - \theta_5) & = & 0 \\
\ddot{\theta}_5 + \frac{g}{l} sin(\theta_5) + a(\theta_5 - \gamma) + b(\theta_5 - \theta_4) & = & 0
\end{array}\right\} \qquad (2.1)$$

where

$$a \equiv \frac{\kappa}{ml^2};\ b \equiv \frac{\widetilde{\kappa}}{ml^2}$$

The next step now is to take a trial solution and substitute it in (2.1). The motion of each pendulum is expected to be oscillatory, so a solution of the following form will be attempted

$$\theta_n = \Theta_n e^{i\omega t}$$

Where ω is the driving frequency and Θ_n can be complex.[3] These trial solutions are complex functions that are being used for their great efficiency. Only the real part of each solution is physically significant, so after the final step of the solution, the real parts of θ_n should be taken, if one is interested in the time dependent solution.

In (2.1), a small angle approximation will be made, resulting in $sin(\theta_n) \approx \theta_n$. Also, it is assumed that the driving motion can be described by $\gamma = \gamma_0 e^{i\omega t}$, where γ_0 is a real number.[4]

Substituting the trial solutions into (2.1) and canceling the common exponential factor yields

$$\left.\begin{array}{rcl}
-\omega^2\Theta_1 + \frac{g}{l}\Theta_1 + a(\Theta_1 - \gamma_0) + b(\Theta_1 - \Theta_2) & = & 0 \\
-\omega^2\Theta_2 + \frac{g}{l}\Theta_2 + a(\Theta_2 - \gamma_0) + b(\Theta_2 - \Theta_1) + b(\Theta_2 - \Theta_3) & = & 0 \\
-\omega^2\Theta_3 + \frac{g}{l}\Theta_3 + a(\Theta_3 - \gamma_0) + b(\Theta_3 - \Theta_2) + b(\Theta_3 - \Theta_4) & = & 0 \\
-\omega^2\Theta_4 + \frac{g}{l}\Theta_4 + a(\Theta_4 - \gamma_0) + b(\Theta_4 - \Theta_3) + b(\Theta_4 - \Theta_5) & = & 0 \\
-\omega^2\Theta_5 + \frac{g}{l}\Theta_5 + a(\Theta_5 - \gamma_0) + b(\Theta_5 - \Theta_4) & = & 0
\end{array}\right\} \qquad (2.2)$$

[2] This is Lagrange's equation when dissipative forces are not considered. Those forces will be considered in section 2.3.

[3] A complex amplitude has a magnitude and a phase, which are the two arbitrary constants necessary in the solution of a second-order differential equation. Thus, the trial solution can be equally written as $\theta_n = |\Theta_n| e^{i(\omega t - \phi_n)}$. When there is no damping, the pendula will either carry a zero or π phase with respect to a sinusoidal driving signal. As a result the amplitude will always be real. Therefore, the complex amplitude is especially useful when a damped system is being considered, because the solution in this case might carry any phase.

[4] The driving amplitude is not allowed to be complex, such that it carries a zero phase. The phases of the pendula are then automatically defined with respect to the driving signal.

This constitutes a set of coupled second order linear differential equations, which allows the introduction of the transformation matrix $\mathbf{M}$. Collecting terms with a common factor Θ_n yields

$$\mathbf{M}\begin{pmatrix}\Theta_1\\ \Theta_2\\ \Theta_3\\ \Theta_4\\ \Theta_5\end{pmatrix} = a\gamma_0\begin{pmatrix}1\\ 1\\ 1\\ 1\\ 1\end{pmatrix} \tag{2.3}$$

where

$$\mathbf{M} \equiv \begin{pmatrix}\beta & -b & 0 & 0 & 0\\ -b & \beta+b & -b & 0 & 0\\ 0 & -b & \beta+b & -b & 0\\ 0 & 0 & -b & \beta+b & -b\\ 0 & 0 & 0 & -b & \beta\end{pmatrix}$$

and

$$\beta \equiv -\omega^2 + \frac{g}{l} + a + b$$

In order to find the amplitude (and phase) response, (2.3) has to be solved for Θ_n. Using Cramer's rule [**?**], the solution is given by

$$\Theta_n = \frac{det(\mathbf{M_n})}{det(\mathbf{M})}$$

where $\mathbf{M_n}$ is the matrix formed by replacing the the n-th column of $\mathbf{M}$ by the vector $a\gamma_0[1\ 1\ 1\ 1\ 1]^T$.

As the simple system (i.e. equal $l, \kappa, \tilde{\kappa}$, and m and without damping) is being considered, an exact solution can be found. This exact solution has been obtained and is found to be

$$\boxed{\Theta_n = \frac{a\gamma_0}{-\omega^2 + \frac{g}{l} + a}} \tag{2.4}$$

2.2 Analyzing the result

The next step in further expanding this theoretical model is to analyze the result so far, to ensure that this derivation is correct and to understand the behaviour that this model describes.

To start, from (2.4), the amplitude $|\Theta_n|$ and the phase response can be plotted against the driving frequency ω. The result of this plot can be found in Figure 2.1.

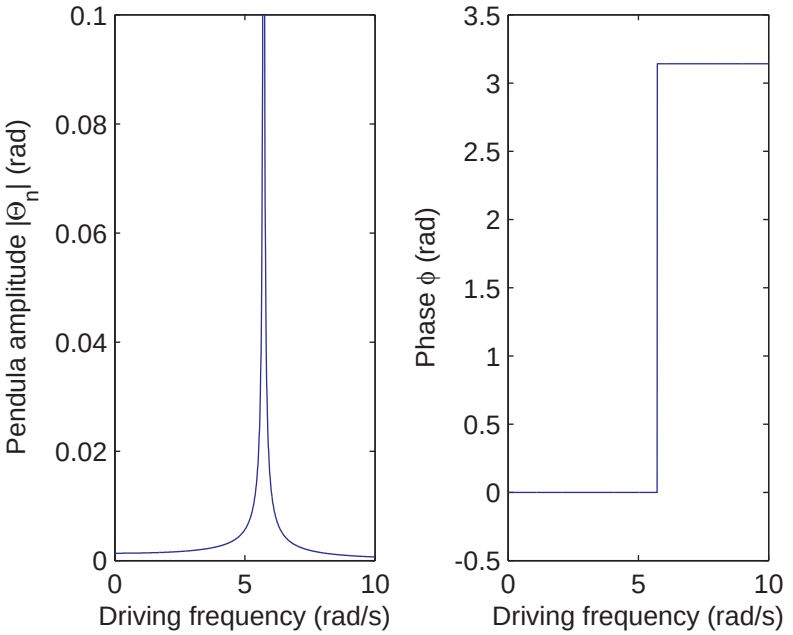

Figure 2.1: Left: Pendula amplitude versus driving frequency γ_0 with equal pendulum lengths and no damping. Right: Pendula phase versus driving frequency γ_0 with equal pendulum lengths and no damping.

This is a somewhat surprising result, as (2.4) is independent of n and b as can also be seen in the amplitude and phase response. Thus it can be concluded that in this case all pendula have the same amplitude response, all have a zero phase shift with respect to each other and they act as if there is no coupling between them. It would appear to be that no matter what the driving frequency is, not all of five expected eigenmodes - that are to be expected since this system has five pendula - can be excited[5]. To better understand this behaviour and to verify that this result is in fact correct, the eigenmodes and eigenfrequencies of this system will now be derived.

2.2.1 Eigenmodes and eigenfrequencies

The eigenmodes and corresponding eigenfrequencies of the system can be found by considering the system without driving (i.e. setting γ_0 to zero), because eigenmodes are characteristics of the system, independent of the system being driven or not. It is expected then, when the system is driven at a certain eigenfrequency, that its corresponding eigenmode will be excited. However, this happens not to be the case.

[5]In fact, it will be shown in the following section that only one eigenmode can be excited and maintained using driving.

The simple system being considered does not include damping, which changes the eigenfrequencies of the system. The degree of damping in an oscillating system is commonly described in terms of the quality factor Q of the system. If the system's quality factor, Q, is large enough, the eigenfrequencies approach those of an undamped oscillator, as will be shown in section 2.2.1.2. Therefore, the eigenmodes and eigenfrequencies of the undamped system will be derived in the following section, followed by a similar derivation for the damped system.

2.2.1.1 Eigenfrequencies and eigenmodes

Finding the eigenmodes of the system is subject to solving

$$\mathbf{M}\begin{pmatrix}\Theta_1\\ \Theta_2\\ \Theta_3\\ \Theta_4\\ \Theta_5\end{pmatrix} = \begin{pmatrix}0\\0\\0\\0\\0\end{pmatrix} \tag{2.5}$$

Equation (2.5) has non-trivial solutions if and only if $det(\mathbf{M}) = 0$. The characteristic equation represented by this determinant is an equation of degree n in ω^2 and its roots might be labelled ω_r^2. The ω_r are the eigenfrequencies of the system and can be shown to be

$$\begin{aligned}
\omega_1 &= \pm\sqrt{\frac{(g+al)}{l}}\\
\omega_2 &= \pm\sqrt{\frac{2g+2al+3bl+\sqrt{5}bl}{2l}}\\
\omega_3 &= \pm\sqrt{\frac{2g+2al+3bl-\sqrt{5}bl}{2l}}\\
\omega_4 &= \pm\sqrt{\frac{2g+2al+5bl+\sqrt{5}bl}{2l}}\\
\omega_5 &= \pm\sqrt{\frac{2g+2al+5bl-\sqrt{5}bl}{2l}}
\end{aligned} \tag{2.6}$$

Note that all of the ω_r are real, as should be the case without damping, or else the total energy of the system would decrease monotonically with the time. As all of the roots are distinct, the system is non-degenerate - that is, every mode is distinguishable. The different eigenmodes follow from subsituting the squared radicals ω_r^2 in (2.5) and solving for the amplitude vector accordingly. They can be shown to be

$$\begin{aligned}
\vec{\eta}_1 &= \begin{pmatrix} 1 \\ 1 \\ 1 \\ 1 \\ 1 \end{pmatrix} & \vec{\eta}_2 &= \begin{pmatrix} -1 \\ \frac{1}{2}(\sqrt{5}+1) \\ 0 \\ -\frac{1}{2}(\sqrt{5}+1) \\ 1 \end{pmatrix} \\
\vec{\eta}_3 &= \begin{pmatrix} -1 \\ -\frac{1}{2}(\sqrt{5}-1) \\ 0 \\ \frac{1}{2}(\sqrt{5}-1) \\ 1 \end{pmatrix} & \vec{\eta}_4 &= \begin{pmatrix} 1 \\ -\frac{1}{2}(\sqrt{5}+3) \\ \sqrt{5}+1 \\ -\frac{1}{2}(\sqrt{5}+3) \\ 1 \end{pmatrix} \\
\vec{\eta}_5 &= \begin{pmatrix} 1 \\ \frac{1}{2}(\sqrt{5}-3) \\ -\sqrt{5}+1 \\ \frac{1}{2}(\sqrt{5}-3) \\ 1 \end{pmatrix}
\end{aligned} \tag{2.7}$$

These eigenvectors constitute an orthogonal set as their inner product is zero, $\langle\vec{\eta}_i|\vec{\eta}_j\rangle = 0$ $(i \neq j)$, which is to be expected, since $\mathbf{M}$ is symmetric. The principle of superposition then applies to the set of linearized differential equations. Thus, the general solution for θ_n must be written as a linear combination of the solutions for each of the k = 5 (where k is the number of oscillators) values of r,

$$\begin{aligned}
\theta_n(t) &= \Theta^+_{n,1}e^{i\omega_1 t} + \Theta^-_{n,1}e^{-i\omega_1 t} + \Theta^+_{n,2}e^{i\omega_2 t} + \Theta^-_{n,2}e^{-i\omega_2 t} + \Theta^+_{n,3}e^{i\omega_3 t} \\
&\quad + \Theta^-_{n,3}e^{-i\omega_3 t} + \Theta^+_{n,4}e^{i\omega_4 t} + \Theta^-_{n,4}e^{-i\omega_4 t} + \Theta^+_{n,5}e^{i\omega_5 t} + \Theta^-_{n,5}e^{-i\omega_5 t} \\
&= \sum_{r=1}^{k} \Theta^+_{n,r}e^{i\omega_r t} + \sum_{r=1}^{k} \Theta^-_{n,r}e^{-i\omega_r t} \\
&= \sum_{r=1}^{k} \left(\Theta^+_{n,r}e^{i\omega_r t} + \Theta^-_{n,r}e^{-i\omega_r t}\right)
\end{aligned}$$

Because it is only the real part of $\theta_n(t)$ that is physically meaningful, the final solution is (see also section 2.1)

$$\theta_n(t) = \Re\left[\sum_{r=1}^{k} \left(\Theta^+_{n,r}e^{i\omega_r t} + \Theta^-_{n,r}e^{-i\omega_r t}\right)\right] = \sum_{r=1}^{k} \left(\Theta^+_{n,r}cos(\omega_r t) + \Theta^-_{n,r}cos(\omega_r t)\right) \tag{2.8}$$

This set of solutions does still have $2k$ arbitrary constants for each equation for θ_n, giving a total of $2k^2 = 50$ unknown arbitrary constants. However, the relation between different $\Theta_{n,r}$ is given by the eigenvectors $\vec{\eta}_r$. Let $\vec{\eta}_{m,r}$ designate the mth component of the rth eigenvector. Then for a given r,

$$\Theta_{1,r} : \Theta_{2,r} : \Theta_{3,r} : \Theta_{4,r} : \Theta_{5,r} = \eta_{1,r} : \eta_{2,r} : \eta_{3,r} : \eta_{4,r} : \eta_{5,r}$$

These relations reduce the number of arbitrary constants with a factor k, namely to $2k = 10$, just as expected, because there are 5 equations of motion that are of second order. The values of these constants are completely specified by the initial conditions of the system.

Equation (2.8) is the homogenous solution. In case of driving with damping, this is then the transient solution and the steady state solution is given by the particular solution. A particular solution would again be of the form $\theta_{n,p} = \epsilon_n e^{i\omega t}$.

2.2.1.2 Effects of damping

In section 2.3 it will be shown how the equations of motion will change when damping (μ) is being included. The results will already be used in this subsection, to elaborate on the eigenfrequencies and eigenmodes of the damped system. The transformation matrix slighty alters with $i\mu w$ added to its diagonal elements

$$\mathbf{M'} = \begin{pmatrix} \beta + i\mu\omega & -b & \cdots & 0 \\ -b & \beta + b + i\mu\omega & \cdots & 0 \\ \vdots & \vdots & \ddots & \vdots \\ 0 & 0 & \cdots & \beta + i\mu\omega \end{pmatrix}$$

with

$$\beta \equiv -\omega^2 + \frac{g}{l} + a + b$$

In a similar way as in subsection 2.2.1.1, the complex eigenfrequencies follow from **M'** as

$$\begin{aligned}
\omega_1 &= \frac{1}{2}\mu i \pm \sqrt{\frac{-\frac{1}{4}\mu^2 l + al + 2g}{l}} \\
\omega_2 &= \frac{1}{2}\mu i \pm \sqrt{\frac{-\frac{1}{2}\mu^2 l + 2g + 2al + 3bl + \sqrt{5}bl}{2l}} \\
\omega_3 &= \frac{1}{2}\mu i \pm \sqrt{\frac{-\frac{1}{2}\mu^2 l + 2g + 2al + 3bl - \sqrt{5}bl}{2l}} \\
\omega_4 &= \frac{1}{2}\mu i \pm \sqrt{\frac{-\frac{1}{2}\mu^2 l + 2g + 2al + 5bl + \sqrt{5}bl}{2l}} \\
\omega_5 &= \frac{1}{2}\mu i \pm \sqrt{\frac{-\frac{1}{2}\mu^2 l + 2g + 2al + 5bl - \sqrt{5}bl}{2l}}
\end{aligned} \tag{2.9}$$

Which reduce to the same eigenfrequencies as (2.6) when there is no damping ($\mu = 0$). It can be shown that the eigenvectors remain unchanged when damping

is included, thus the same set of eigenvectors given by (2.7) applies.

In case of damping, it is the real part of ω_r which determines the angular frequency of the oscillatory motion. The imaginary part of ω_r produces terms of the form $e^{-\Im(\omega_r)t}$ in the expression for $\theta_n(t)$ and therefore determines the rate at which energy is being dissipated from the system.

If the Q-factor of the system is high enough, this will yield a small value for μ, such that μ^2 will be negligible, resulting in unchanged eigenfrequencies compared to the undamped system. Experiments have been done on the pendulum, and they are discussed in Chapter 4. It will be shown in that Chapter, that the Q-factor for a single uncoupled pendulum will be around 28, which is fairly high. Therefore, in general, damping cannot be neglected as it will influence the behaviour of the system, but it does not have a profound effect on the eigenfrequencies of the system.

2.2.1.3 The eigenmode paradox

Different simulations were performed for the system being driven at one of the values of ω_r. It became evident soon, that only one of the five calculated eigenmodes could be excited and maintained, for both the system with and without damping. This was eigenmode $\vec{\eta}_1$, the mode in which every pendulum has the same amplitude and phase. The reason for this happening can be explained by considering one of the other eigenmodes - say, $\vec{\eta}_2$ - and observing what happens when the system is being driven at the accompanying resonance frequency ω_2. For simplicity, no coupling between pendula will be considered intially, meaning that $b = 0$. See Figure 2.2 for a schematic respresentation of the maximum amplitudes of eigenmode $\vec{\eta}_2$.

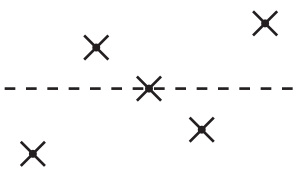

Figure 2.2: Schematic representation of eigenmode $\vec{\eta}_2$. The dotted line indicates zero amplitude.

As can clearly be observed from the figure, this eigenmode is completely symmetric - meaning that pendula 1 and 5 have the same amplitude but opposite phase, pendula 2 and 4 also have the same amplitude but opposite phase and pendulum 3 does not deviate from its equilibrium. If the set-up was put in that initial condition of the eigenmode, experienced no damping and was left undriven, it would remain in this eigenmode for all eternity and in the case of damping, this eigenmode would obviously die out after a said period of time. Adding driving to this eigenmode, however, complicates things. It is therefore wise to once again schematically represent what happens when driving is added to the equation. See Figure 2.3 for a schematic representation of this eigenmode,

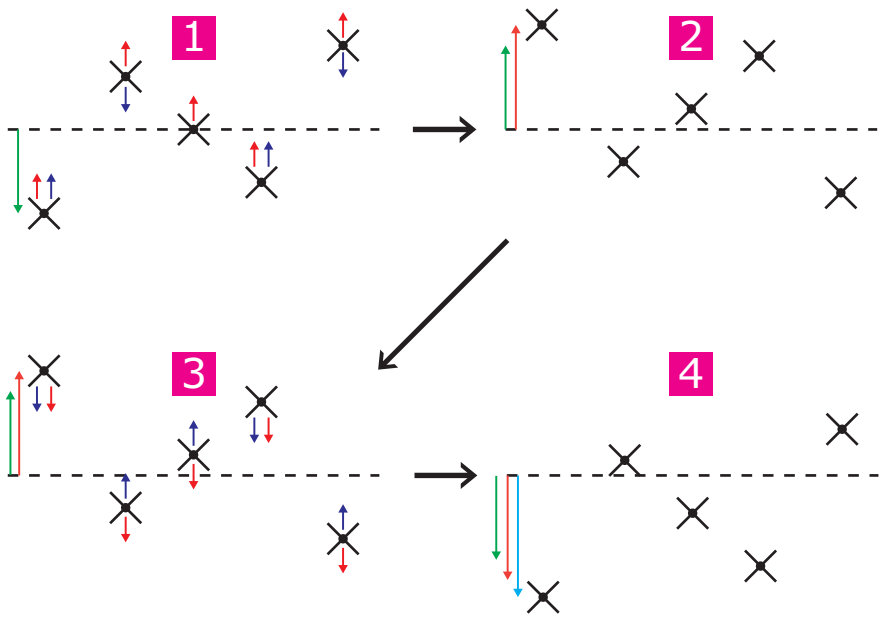

Figure 2.3: Schematic representation of the forces on the different pendula in eigenmode η_2 in the case of driving at different moments in the drive cycle.

in the case of driving.

In part 1 of this figure, the set-up is placed in the initial conditions of eigenmode $\vec{\eta}_2$. The green arrow next to the left-most pendulum graphically represents the maximum amplitude of this particular pendulum. At exactly this moment, the drive axle is brought in motion. The red arrows indicate the direction in which the drive axle is then turning - this is arbitrarily chosen upward to begin with - and also indicate the force that is (indirectly) exerted on each pendulum by the drive axle. The blue arrows represent the direction in which each pendulum would move if undriven.

After half a period of the drive motion, the situation of the system will then be as presented in part 2 of the figure. The pendula that were below the dotted line in part 1 of the figure were pushed beyond their undriven maximum amplitude by the motion of the drive axle, whereas the pendula below the dotted line were slowed down and now have an amplitude that is less than their undriven maximum amplitude. To illustrate that the amplitude of the left-most pendulum has increased, a pink arrow was drawn alongside the original green arrow to indicate the new amplitude of that pendulum.

In the second part of the motion of the drive axle, the forces on each pendulum will now be in the opposite direction and are represented in part 3 of the figure. Following the same reasoning as before, part 4 of the figure indicates the situation after a full drive cycle was completed and a clear picture can be formed as to what will happen with the entire system if this motion will take

place for a long period of time. Again, the green and pink arrows together with a new blue arrow were added to illustrate that the amplitude of the left-most pendulum has increased after a full drive cycle.

The motion of this particular eigenmode will obviously die out as the pendula that initially move in-phase with the motor will be accelerated and the pendula that are π rad out of phase will be slowed down. In the case where there is no coupling between pendula, the out-of-phase pendula will simply slow down, and then start to move in-phase with the motor, meaning that all pendula will eventually swing in-phase with each other. Since there is no coupling, $b = 0$ and $\omega_2 = \omega_1$- this follows from (2.6) - and the systems motion will explode[6]. In the case where coupling between pendula *is* being considered, the motion is all but simple and beating will occur as the energy will be redistributed evenly across all pendula, meaning that after a transient period the pendula will eventually swing in-phase and all with the same finite amplitude - as in this case $\omega_2 \neq \omega_1$ and the system will therefore not explode.

This conclusion can now be extended to each of the different eigenmodes of this system, yielding that in the driven case, none but eigenmode $\vec{\eta}_1$ can be excited when the system is being driven at the eigenfrequencies belonging to the respected eigenmodes, as was predicted by (2.4), ensuring that this model is in fact correct so far.

2.3 The extended system

In section 2.1, a theoretical model of the experimental set-up was derived which does not include damping, different lengths and masses of the pendula or different spring constants. In the experimental set-up, these parameters may differ significantly, causing behaviour that the basic theoretical model cannot reproduce. Since this model should accurately describe the behaviour of the experimental set-up, all of these different parameters should be included in the theoretical model. In this section it will be described how this is done.

2.3.1 Damping

In Lagrangian mechanics, the Rayleigh dissipation function can be used to include viscous forces and thus damping[3]. The definition of the Rayleigh dissipation function is given by

$$D = \frac{1}{2} \sum_{j=1}^{\widetilde{m}} \sum_{k=1}^{\widetilde{m}} \mu_{jk} \dot{\theta}_j \dot{\theta}_k \tag{2.10}$$

[6] In this ideal linear, uncoupled system, the relative phase between the drive signal and the system is 0 rad for $\omega < \omega_1$ and is π rad for $\omega > \omega_1$. The phase will be $\frac{1}{2}\pi$ rad only at exactly $\omega = \omega_1$. If the phase is zero, the axle-coupling springs are not stretched and will exert no force on the pendula. If the phase is π rad, the motor will exactly counteract the movement of the pendulum, also resulting in no net force or addition of energy. Only at exactly $\omega = \omega_1$, the motor can continuously drive the system and thus add energy continuously. If no damping is being considered, the energy has nowhere to go, so the amplitudes blow up.

Where $\widetilde{m}$ denotes the total amount of generalized coordinates in a system (in this case five), $\dot{\theta}_j$ and $\dot{\theta}_j$ denote the time derivatives of the generalized coordinates and μ_{jk} are damping constants.

Equation (2.10) suggests that there are viscous forces that depend on the velocities of the different pendula and even on the relative velocities between pendula. In the experimental set-up, the coupling between neighbouring pendula is quite small when compared to the coupling between the pendula and the driving axle - the spring constants of the pendulum-coupling springs are roughly ten times smaller. Therefore, it is assumed that the damping constants μ_{jk} for $j \neq k$ are negligible and these terms can be ignored in the dissipation function. Furthermore, it is assumed that damping due to air friction is significantly larger than damping due to dissipation of heat in for example the axle-coupling springs or the ball bearings. This results in $\mu_{jk} = \mu$ for each value of j and k.

The aforementioned then implies that the dissipation function for this system is given by

$$D = \frac{1}{2}\mu(\dot{\theta}_1^2 + \dot{\theta}_2^2 + \dot{\theta}_3^2 + \dot{\theta}_4^2 + \dot{\theta}_5^2) \tag{2.11}$$

In the case of damping, Lagranges equation per pendulum is now given by

$$\frac{\partial}{\partial t}\left(\frac{\partial L}{\partial \dot{\theta_n}}\right) - \frac{\partial L}{\partial \theta_n} + \frac{\partial D}{\partial \dot{\theta_n}} = 0$$

Which, including (2.11), then yields

$$\begin{array}{rcl}
\ddot{\theta}_1 + \frac{g}{l}sin(\theta_1) + a(\theta_1 - \gamma) + b(\theta_1 - \theta_2) + \mu\dot{\theta}_1 & = & 0 \\
\ddot{\theta}_2 + \frac{g}{l}sin(\theta_2) + a(\theta_2 - \gamma) + b(\theta_2 - \theta_1) + b(\theta_2 - \theta_3) + \mu\dot{\theta}_2 & = & 0 \\
\ddot{\theta}_3 + \frac{g}{l}sin(\theta_3) + a(\theta_3 - \gamma) + b(\theta_3 - \theta_2) + b(\theta_3 - \theta_4) + \mu\dot{\theta}_3 & = & 0 \\
\ddot{\theta}_4 + \frac{g}{l}sin(\theta_4) + a(\theta_4 - \gamma) + b(\theta_4 - \theta_3) + b(\theta_4 - \theta_5) + \mu\dot{\theta}_4 & = & 0 \\
\ddot{\theta}_5 + \frac{g}{l}sin(\theta_5) + a(\theta_5 - \gamma) + b(\theta_5 - \theta_4) + \mu\dot{\theta}_5 & = & 0
\end{array}$$

Linearizing and filling in the same trial solution as before, this yields

$$\begin{array}{rcl}
-\omega^2\Theta_1 + \frac{g}{l}\Theta_1 + a(\Theta_1 - \gamma_0) + b(\Theta_1 - \Theta_2) + i\omega\mu\Theta_1 & = & 0 \\
-\omega^2\Theta_2 + \frac{g}{l}\Theta_2 + a(\Theta_2 - \gamma_0) + b(\Theta_2 - \Theta_1) + b(\Theta_2 - \Theta_3) + i\omega\mu\Theta_2 & = & 0 \\
-\omega^2\Theta_3 + \frac{g}{l}\Theta_3 + a(\Theta_3 - \gamma_0) + b(\Theta_3 - \Theta_2) + b(\Theta_3 - \Theta_4) + i\omega\mu\Theta_3 & = & 0 \\
-\omega^2\Theta_4 + \frac{g}{l}\Theta_4 + a(\Theta_4 - \gamma_0) + b(\Theta_4 - \Theta_3) + b(\Theta_4 - \Theta_5) + i\omega\mu\Theta_4 & = & 0 \\
-\omega^2\Theta_5 + \frac{g}{l}\Theta_5 + a(\Theta_5 - \gamma_0) + b(\Theta_5 - \Theta_4) + i\omega\mu\Theta_5 & = & 0
\end{array}$$

Which is the same as (2.2) when there is no damping ($\mu = 0$).

2.3.2 Pendula lengths and masses

By far the most obvious parameter that can be changed in the experimental set-up is the length of a particular pendulum. Less obvious but still relevant is the fact that their masses will differ as well.

By assuming different lengths l_n and different masses m_n and deriving the equations leading up to (2.2), this will yield

$$\begin{array}{rcl}
-\omega^2\Theta_1 + \frac{g}{l_1}\Theta_1 + a_1(\Theta_1 - \gamma_0) + b_1(\Theta_1 - \Theta_2) + i\omega\mu\Theta_1 & = & 0 \\
-\omega^2\Theta_2 + \frac{g}{l_2}\Theta_2 + a_2(\Theta_2 - \gamma_0) + b_2(\Theta_2 - \Theta_1) + b_2(\Theta_2 - \Theta_3) + i\omega\mu\Theta_2 & = & 0 \\
-\omega^2\Theta_3 + \frac{g}{l_3}\Theta_3 + a_3(\Theta_3 - \gamma_0) + b_3(\Theta_3 - \Theta_2) + b_3(\Theta_3 - \Theta_4) + i\omega\mu\Theta_3 & = & 0 \\
-\omega^2\Theta_4 + \frac{g}{l_4}\Theta_4 + a_4(\Theta_4 - \gamma_0) + b_4(\Theta_4 - \Theta_3) + b_4(\Theta_4 - \Theta_5) + i\omega\mu\Theta_4 & = & 0 \\
-\omega^2\Theta_5 + \frac{g}{l_5}\Theta_5 + a_5(\Theta_5 - \gamma_0) + b_5(\Theta_5 - \Theta_4) + i\omega\mu\Theta_5 & = & 0
\end{array}$$

Where now

$$a_n \equiv \frac{\kappa}{m_n l_n^2};\ b_n \equiv \frac{\widetilde{\kappa}}{m_n l_n^2}$$

2.3.3 Spring constants

The final contributing factor in the experimental set-up that will be considered is the variation between spring constants. In the experimental set-up they may vary by as much as 60 percent for the pendulum-coupling springs and by 30 percent for the axle-coupling springs - not exactly insignificant. Their addition to the theoretical description together with the previously added parameters now transform (2.2) to assume the following form

$$\left.\begin{array}{rcl}
-\omega^2\Theta_1 + \frac{g}{l_1}\Theta_1 + a_1(\Theta_1 - \gamma_0) + b_1(\Theta_1 - \Theta_2) + i\omega\mu\Theta_1 & = & 0 \\
-\omega^2\Theta_2 + \frac{g}{l_2}\Theta_2 + a_2(\Theta_2 - \gamma_0) + b_2(\Theta_2 - \Theta_1) + b_3(\Theta_2 - \Theta_3) + i\omega\mu\Theta_2 & = & 0 \\
-\omega^2\Theta_3 + \frac{g}{l_3}\Theta_3 + a_3(\Theta_3 - \gamma_0) + b_4(\Theta_3 - \Theta_2) + b_5(\Theta_3 - \Theta_4) + i\omega\mu\Theta_3 & = & 0 \\
-\omega^2\Theta_4 + \frac{g}{l_4}\Theta_4 + a_4(\Theta_4 - \gamma_0) + b_6(\Theta_4 - \Theta_3) + b_7(\Theta_4 - \Theta_5) + i\omega\mu\Theta_4 & = & 0 \\
-\omega^2\Theta_5 + \frac{g}{l_5}\Theta_5 + a_5(\Theta_5 - \gamma_0) + b_8(\Theta_5 - \Theta_4) + i\omega\mu\Theta_5 & = & 0
\end{array}\right\} \quad (2.12)$$

Where now

$$\begin{array}{rcl}
a_n & \equiv & \frac{\kappa_n}{m_n l_n^2};\ b_1 \equiv \frac{\widetilde{\kappa}_1}{m_1 l_1^2};\ b_2 \equiv \frac{\widetilde{\kappa}_1}{m_2 l_2^2};\ b_3 \equiv \frac{\widetilde{\kappa}_2}{m_2 l_2^2};\ b_4 \equiv \frac{\widetilde{\kappa}_2}{m_3 l_3^2} \\
b_5 & \equiv & \frac{\widetilde{\kappa}_3}{m_3 l_3^2};\ b_6 \equiv \frac{\widetilde{\kappa}_3}{m_4 l_4^2};\ b_7 \equiv \frac{\widetilde{\kappa}_4}{m_4 l_4^2};\ b_8 \equiv \frac{\widetilde{\kappa}_4}{m_5 l_5^2}
\end{array}$$

Taking all of these new parameters into consideration, (2.12) can be solved using Cramer's rule for each independent Θ_n as before in section 2.1.

Chapter 3

Constructing the simulation model

In order to be able to predict the behaviour of the system, the next step is to make a simulation model that can receive an arbitrary drive input signal and presents the response of the system, $\theta_n(t)$. Initially, a model was built in Simulink for its easy implementation, but quickly thereafter it became apparent that Simulink was not the best choice for our needs as it required more steps to change variables and process the results than is necessary. Therefore, a more complete model was built in MATLAB using its built-in ODE45 functionality. This chapter will briefly discuss how both the Simulink and MATLAB models were built.

3.1 Simulink

To build this model, (3.1) was taken and each of the equations was rewritten for $\ddot{\theta}_n$. Then, using integrators, $\dot{\theta}_n$ and θ_n could easily be calculated using Simulink. For example, see Figure 3.1 for the Simulink subsystem of pendulum 1. The same procedure was followed for all other pendula and the subsystems were connected so that the complete system was now described in Simulink.

$$\left.\begin{array}{lcl}
\ddot{\theta}_1 + \frac{g}{l_1} sin(\theta_1) + a_1(\theta_1 - \gamma) + b_1(\theta_1 - \theta_2) + \mu\dot{\theta}_1 & = & 0 \\
\ddot{\theta}_2 + \frac{g}{l_2} sin(\theta_2) + a_2(\theta_2 - \gamma) + b_2(\theta_2 - \theta_1) + b_3(\theta_2 - \theta_3) + \mu\dot{\theta}_2 & = & 0 \\
\ddot{\theta}_3 + \frac{g}{l_3} sin(\theta_3) + a_3(\theta_3 - \gamma) + b_4(\theta_3 - \theta_2) + b_5(\theta_3 - \theta_4) + \mu\dot{\theta}_3 & = & 0 \\
\ddot{\theta}_4 + \frac{g}{l_4} sin(\theta_4) + a_4(\theta_4 - \gamma) + b_6(\theta_4 - \theta_3) + b_7(\theta_4 - \theta_5) + \mu\dot{\theta}_4 & = & 0 \\
\ddot{\theta}_5 + \frac{g}{l_5} sin(\theta_5) + a_5(\theta_5 - \gamma) + b_8(\theta_5 - \theta_4) + \mu\dot{\theta}_5 & = & 0
\end{array}\right\} \quad (3.1)$$

As an input for this Simulink model, initially a sine signal was added. This meant that ω and γ_0 could be adjusted and the system could be run for a predefined amount of time. A graph was added which plotted θ_n as a function of time.

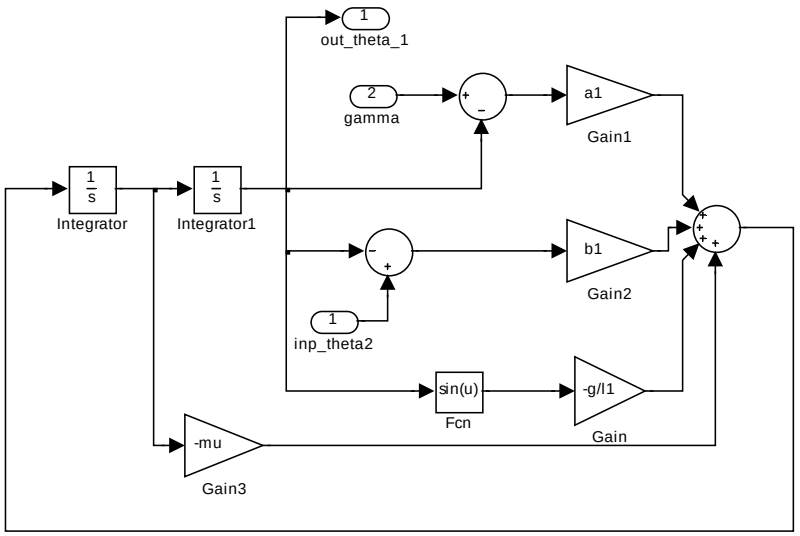

Figure 3.1: Simulink subsystem of pendulum 1

In the end, this model worked as expected and yielded proper results. For example, it could be observed that when all pendula had equal lengths, the amplitudes were all the same, no eigenmodes could be excited and at resonance frequency their amplitude grew enormously.

3.2 MATLAB

The set of differential equations given by (2.12), can be numerically solved by MATLAB using the ODE45 function that integrates over time. Even though this function can only handle a set of first order differential equations, the set of second order differential equations of can be solved by rewriting it as a system of first order coupled differential equations, see (3.2).

An advantage of solving it numerically, is that now every type of function for $\gamma(t)$ might be imposed on the set of equations. A MATLAB file has been programmed that solves these differential equations subject to its boundary conditions, and plots $\theta_n(t)$. See Appendix B for the accompanying MATLAB files.

$$\left.\begin{array}{lcl}
\dot{\theta}_1 &=& \omega_1 \\
\dot{\theta}_2 &=& \omega_2 \\
\dot{\theta}_3 &=& \omega_3 \\
\dot{\theta}_4 &=& \omega_4 \\
\dot{\theta}_5 &=& \omega_5 \\
\dot{\omega}_1 &=& a_1\gamma(t) - \frac{g}{l_1}sin(\theta_1) - a_1\theta_1 - b_1(\theta_1 - \theta_2) - \mu\omega_1 \\
\dot{\omega}_2 &=& a_2\gamma(t) - \frac{g}{l_2}sin(\theta_2) - a_2\theta_2 - b_2(\theta_2 - \theta_1) - b_3(\theta_2 - \theta_3) - \mu\omega_2 \\
\dot{\omega}_3 &=& a_3\gamma(t) - \frac{g}{l_3}sin(\theta_3) - a_3\theta_3 - b_4(\theta_3 - \theta_2) - b_5(\theta_3 - \theta_4) - \mu\omega_3 \\
\dot{\omega}_4 &=& a_4\gamma(t) - \frac{g}{l_4}sin(\theta_4) - a_4\theta_4 - b_6(\theta_4 - \theta_3) - b_7(\theta_4 - \theta_5) - \mu\omega_4 \\
\dot{\omega}_5 &=& a_5\gamma(t) - \frac{g}{l_5}sin(\theta_5) - a_5\theta_5 - b_8(\theta_5 - \theta_4) - \mu\omega_5
\end{array}\right\} \quad (3.2)$$

To illustrate the output of this model, an example output where the lengths, masses and spring constants are chosen the same is shown in Figure 3.2.

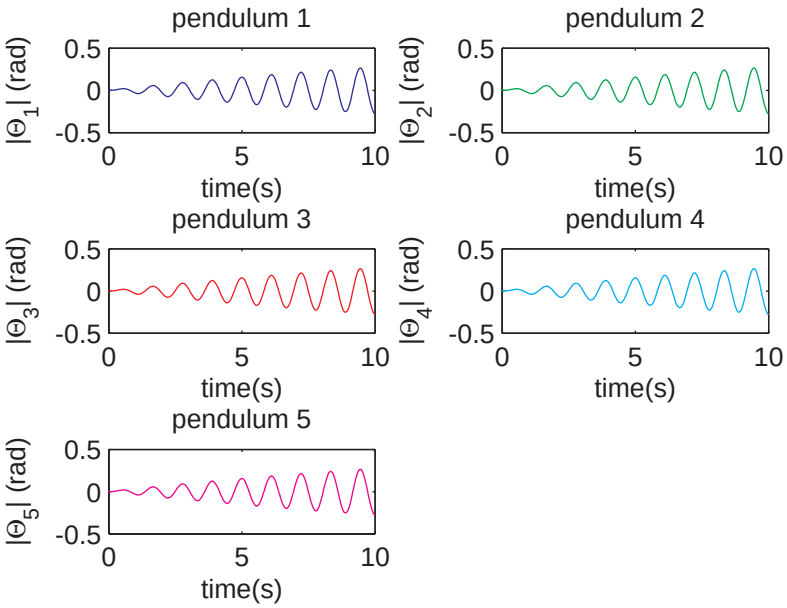

Figure 3.2: Output of the ODE45 model.

One important benefit of this particular model is that it can be chosen to adopt the linear approximation or the non-linear approximation, if desired.

In Chapter 4 pulses will be defined that will drive the system. These pulses are computed discretely and are therefore only defined on certain time points, say t_n, yielding $dt = t_{n+1} - t_n$. When ODE45 is solving the differential equations, it will calculate an optimal time step such that the spacing between successive time points will not be equal. Problem is then that the pulse is undefined at the time points generated by ODE45, because they do not match t_n. To avoid this problem, a cubic spline interpolant is being used to interpolate between two points.

Chapter 4

Validating the simulation model

A critical step in designing a simulation model is verifying its validity before predictions can be made using it. In order to verify the validity of the simulation model that was derived in the previous chapter, both the simulation model and the experimental set-up were exposed to an iterative test to (indirectly) measure the maximum amplitudes of the pendula as a function of varying driving frequencies. If these responses are - at least qualitatively - similar, this will demonstrate the validity of the simulation model.

In the end, to demonstrate that this model can now also be used to predict the behaviour of the experimental system, the lengths of some pendula will be altered and the simulation result will be compared to the experimental result.

4.1 The testing procedure

The goal is to drive the pendula with a continuous sinusoidal signal $\gamma = \gamma_0 cos(\omega t)$ where ω is iteratively increased from small to large frequencies. The pendula will initially all be at rest. In the simulation model and the experimental set-up the lengths of the different pendula will be chosen the same and are (for pendula 1 through 5) $0.10m$, $0.15m$, $0.20m$, $0.25m$ and $0.30m$ respectively. After a transitional period, the motion of the pendula will become stable, meaning the transient behaviour has died out and the maximum amplitude of each pendulum can be determined. In this case it is imperative that the driving amplitude γ_0 will be small enough to ensure linear motion. Even though in the end the amplitudes will not quantitatively match[1], the frequencies at which different pendula start to resonate should match.

[1] See section 4.1.2

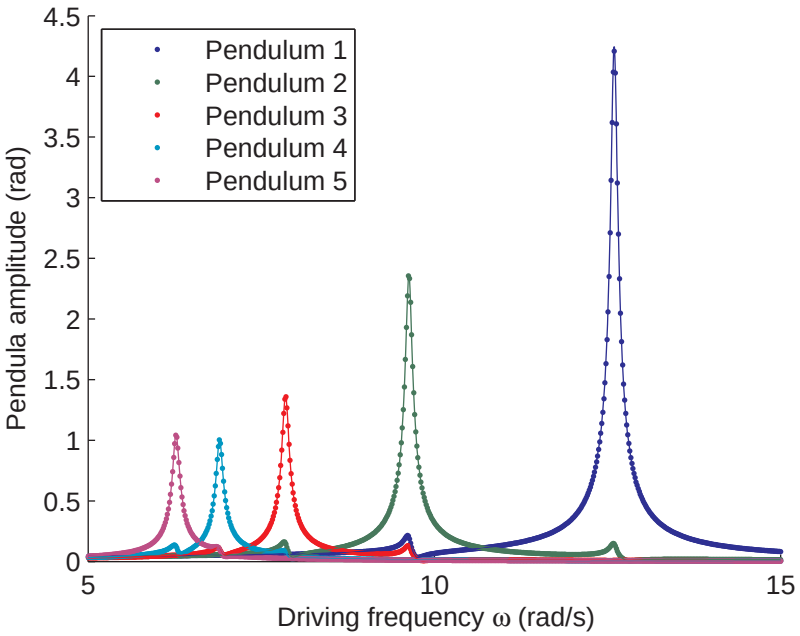

Figure 4.1: Maximum pendulum amplitude as a function of the driving frequency. The solid lines represent analytical data and the dotted lines indicate simulation data.

4.1.1 Simulation model

The simulation model was programmed to recieve the desired continuous sinusoidal input as the drive signal. Linearity is assumed, so the driving amplitude can be arbitrarily chosen - here it was chosen to be $\gamma_0 = 0.1$ rad. All other parameters in the simulation model will be chosen as they were determined in [?]. As will be shown in section 4.1.3, the damping constant is determined to be $\mu = 0.1$ and will be used here for a best approximation. The simulation was driven for a sufficiently long time for the motion to become stable - roughly 150 seconds. In that case the maximum amplitude can safely be determined.

The result of this test can be seen in Figure 4.1. To illustrate that this result is correct, the previously determined analytical response from section 2.1 was added to the same graph.

It can be observed that both responses are in excellent agreement with each other. Because the drive input is a cosine, there is a nonzero amplitude at $\omega = 0$, and for all other frequencies the graphs match very well, meaning that this method is perfect for testing the validity of the theoretical model by performing the same measurement on the experimental set-up and comparing both outcomes.

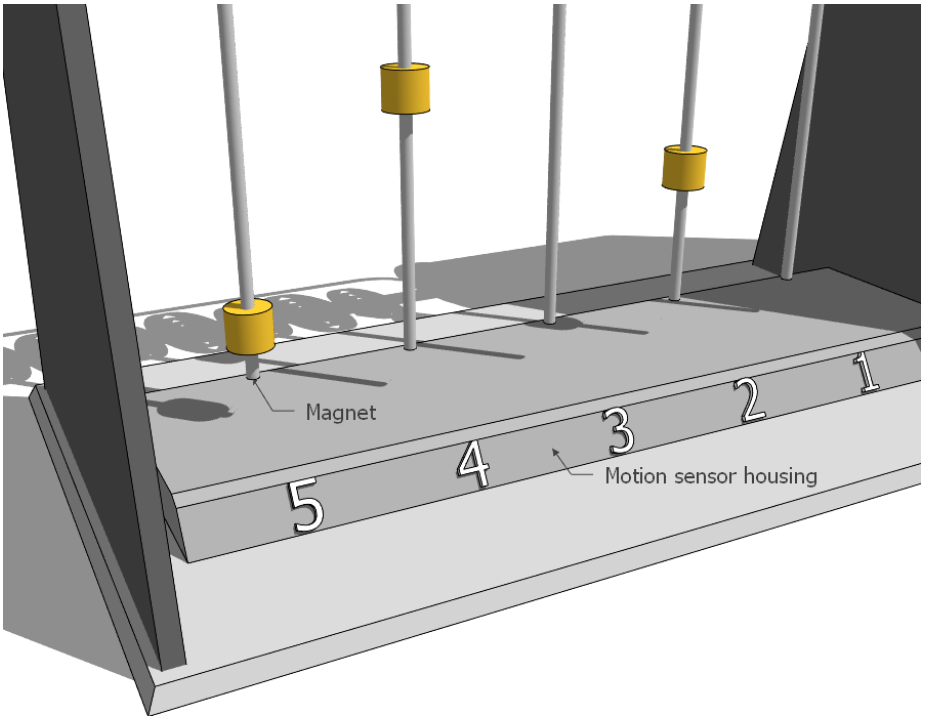

Figure 4.2: Close-up of the motion sensor housing and the magnets on the ends of the pendula

4.1.2 Experimental set-up

In the case of the experimental set-up, determining the maximum amplitude of a pendulum is not directly possible. Instead, the set-up features magnetic flux sensors in the motion sensor housing and small magnets attached to the end of each pendulum, see Figure 4.2. This way the magnetic flux as a function of time is measured, which can be interpreted as the velocity of the pendulum. If a large magnetic flux is measured, this will indicate that the pendulum was moving at a high velocity, which means that the pendulum in turn had a large amplitude. Therefore, if the pendula are driven for a sufficiently long time for the motion to become stable and the peak-to-peak voltage is determined during this stable period, it will be proportional to the maximum amplitude measured in the simulation model - only this time in volts.

Because the simulation model assumes linearity of the system, the driving amplitude is chosen to be as small as possible. As is visible in Figure 4.1, the predicted maximum amplitude at resonance frequencies could exceed π rad, which would cause anything but linear behaviour in the system. If chosen sufficiently small, the experimental set-up is expected to behave approximately linear and the best comparison can be made between both results.

The experimental set-up was driven by a continuous sinusoidal signal for 160 periods of that particular signal. It was determined experimentally that the motion of the pendula was then fairly stable and the peak-to-peak voltage could safely be determined. After each measurement, the pendula were left to slow down, after which the frequency would be increased and another measurement could be performed. Since the simulation model predicts that the resonance frequencies lie between 5 and 15 rad/s, the experimental set-up was driven for frequencies in that same range.

The result of the measurement can be seen in Figure 4.3.

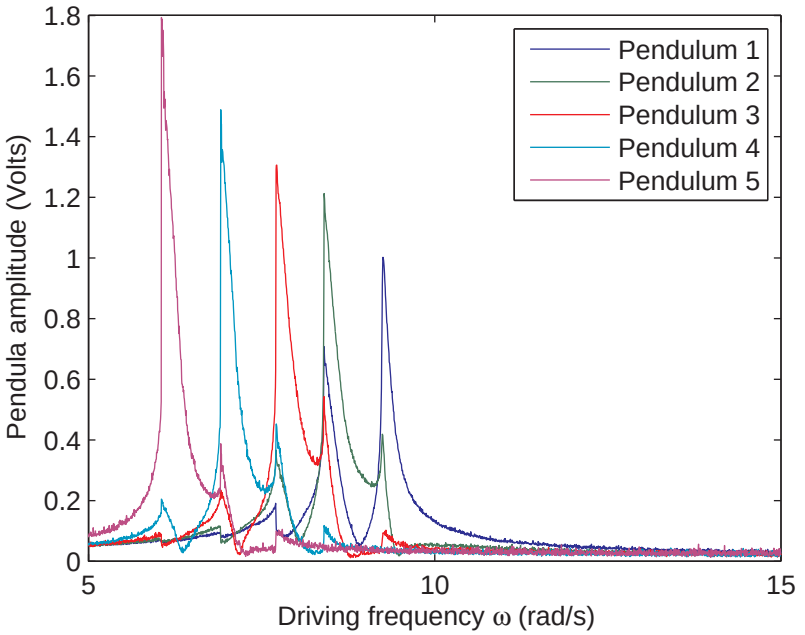

Figure 4.3: Result of experimental measurements.

The most obvious difference between this result and the previously determined analytical one is that the resonance frequencies for pendula which have short lengths lie far from the predicted frequencies but that the resonance frequencies for the pendula with longer lengths match fairly well. Since the lengths of the pendula influence the position of the resonance frequencies greatly, additional testing was performed to determine the lengths of the pendula more accurately.

To do this, each pendulum was disconnected from all springs, ensuring it could swing freely. It was then left to swing for a certain period and the amount of full-period swings in this period was counted. From this, the period of swing T could be determined and using the well known equation for the period of swing, $T \approx 2\pi\sqrt{l/g}$, one can then determine l. This resulted in $l_1 \approx 0.155$ m, $l_2 \approx 0.183$

m, $l_3 \approx 0.205$ m, $l_4 \approx 0.248$ m and $l_5 \approx 0.311$ m. Using these corrected lengths in the model results in a much better prediction of the resonance frequencies. See Figure 4.4.

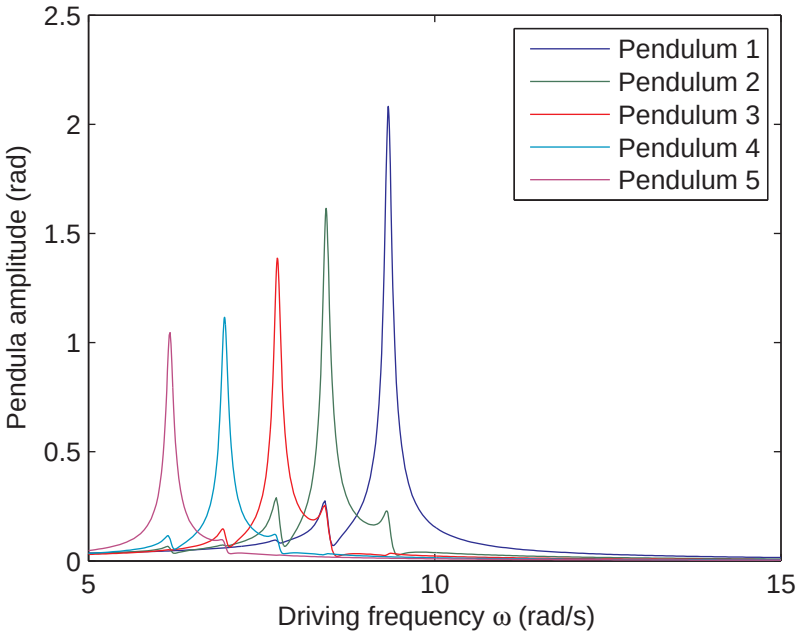

Figure 4.4: Pendulum amplitudes versus driving frequency ω with adjusted pendulum lengths using the simulation model

Another difference between the simulation and the experimental measurements is that the resonance peaks are nonsymmetric in the case of the experimental set-up. Approaching from the left, the amplitude per pendulum increases quite abruptly as the resonance frequency of that particular pendulum is reached, whereas to the right of the resonance frequency the pendulum maintains a relatively large amplitude, even for frequencies far from the resonance frequency. This nonsymmetry is very typical of nonlinear behaviour. To illustrate this further, simulations were performed where in one case linearity was assumed and in the other it was not. See Figure 4.5 for the result.

It is clearly visible that in the case of linearity, the peaks are symmetric, whereas in the case of non-linearity they are not and - although due to the extreme driving amplitude are exaggerated - resemble the experimental data. This is not unsurprising since even at small amplitudes, non-linearity is very much present in the experimental set-up. For a non-linear pendulum it is already well established that the following equation holds for the period of swing

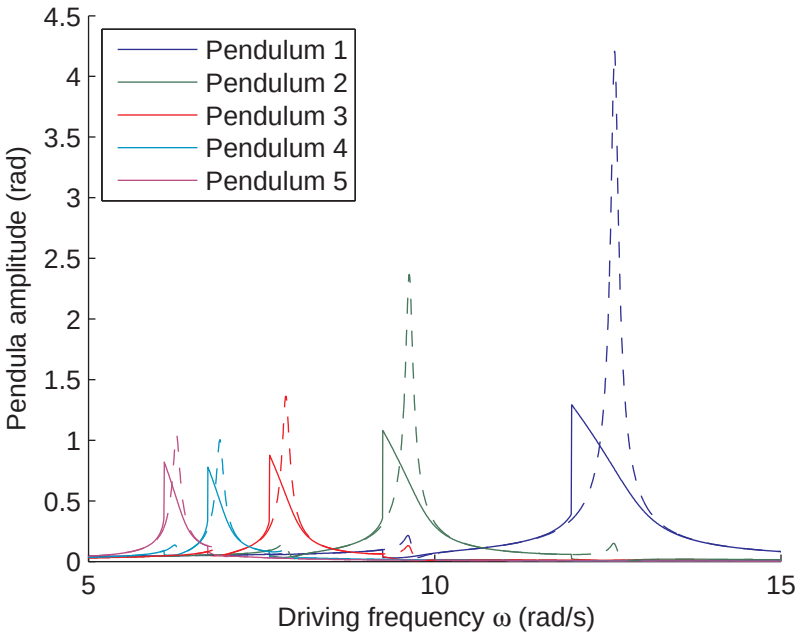

Figure 4.5: Pendula amplitudes versus driving frequency for linear and non-linear assumptions. The solid lines represent non-linear assumptions and the dashed lines represent linear assumption.

$$T = 2\pi\sqrt{\frac{l}{g}}(1 + \frac{1}{16}\theta_0^2 + \frac{11}{3072}\theta_0^4 + \cdots)$$

Even though this equation does not hold exactly in the case of a coupled pendulum, it might be expected that the dependence on θ_0 will also be present in the coupled case. This equation then implies that as the maximum amplitude of a non-linear pendulum increases, the amplitude response appears to shift to the *left* in the frequency domain[2]. The amount of shift is a function of higher order terms of θ_0. This means that as θ_0 increases more and more, so does the shift to the left in the frequency domain of the amplitude response. Eventually, the shift will be so great that the resonance frequency, originally at ω_r is now shifted to the left to a particular value of ω. The pendulum will therefore resonate, but at a frequency lower than the resonance frequency expected from the linear model! As the pendulum still has a large θ_0, but after resonating will decrease again - in the linear amplitude response it has "gone over the top" - the shift will decrease, meaning that the amplitude response shift becomes *less*. But here's the catch: θ_0 decreases so it might be expected that the response might be similar to what

[2]This follows from the fact that the resonance frequency of a pendulum is given by $\omega_0 = 2\pi/T$

was seen approaching from the left in the frequency domain - a quick increase at first, so now a quick decrease. However, since θ_0 decreases, the shift to the left of the amplitude response will also decrease, meaning that the maximum amplitude will decrease less quickly. The shift will then slowly decrease until at higher frequencies θ_0 becomes small enough so that the shift is virtually zero again and matches the linear approximation.

Another difference between both results is that in the theoretical case the peak amplitudes increase as ω is increased, whereas in the experimental measurements it can be observed that they in fact decrease as ω is increased. As the frequency in the driving software was increased, it was observed that the maximum amplitude of the drive axle actually decreased. Of course, the amplitude should remain the same if a proper comparison is to be made between the theoretical and experimental set-up. When the driving amplitude γ_0 decreases, so will the maximum amplitude of a pendulum. Apparently, as ω increases, γ_0 decreases faster than the maximum amplitudes of the pendula would increase, if γ_0 remained constant as function of frequency. This then results in a net decrease of the maximum amplitudes of the pendula as ω increases, as was observed.

The fact that the maximum amplitudes of the pendula in the theoretical case increase is due to the fact that for constant γ_0, the torque exerted on the pendula by the drive axle, τ, remains constant for all ω. From $\frac{\partial^2\theta}{\partial t^2} = \frac{\tau}{ml^2}$, it then follows that shorther pendula have a larger angular acceleration, meaning that their maximum amplitudes will be larger.

The last major difference between both results is that there appears to be a stronger coupling force between pendula, especially for pendula with shorter lengths. In testing the simulation model, it was found that altering the values of the coupling constants of the pendulum-couplinig springs by a relatively small amount affects the response of the system greatly. It could be that due to the self-made nature of the springs that although their properties were as measured at first, over time their response has changed, causing this behaviour.

4.1.3 Estimation of the damping constant

As was discussed in section 4.1.1, most of the parameters in the system have already been determined in previous reports or can easily be measured - all except for the damping constant μ. In this section, an value for μ will be determined for completeness, where the experimental results found in the previous section will be used for the determination.

To begin, in section 2.2.1.2, the quality factor was already briefly mentioned. The Q-factor for a single resonator is given by [3]

$$Q \equiv \frac{m\omega_{resonance}}{\mu}$$

For an uncoupled pendulum, but connected with a spring to the drive axle, the

eigenfrequency is given by

$$\omega_0 = \sqrt{\frac{g}{l} + a}$$

Subsituting this yields

$$\boxed{\mu = \frac{m\sqrt{\frac{g}{l} + a}}{Q}} \tag{4.1}$$

All parameters in (4.1) are known, except for Q. Since the system has been observed to be underdamped, it is expected that the system is a high-Q system. Therefore, the following equation for determining Q may be used

$$Q = \frac{\omega_0}{\Delta\omega}$$

where $\Delta\omega$ is the width of the amplitude curve at half of its maximum amplitude. Since this system is coupled, the Q-factors of all five pendula will be determined and averaged to provide a rough estimate of the Q-factor of the entire system. See Figure 4.6 for an example of how ω_0 and $\Delta\omega$ was determined for pendulum 5.

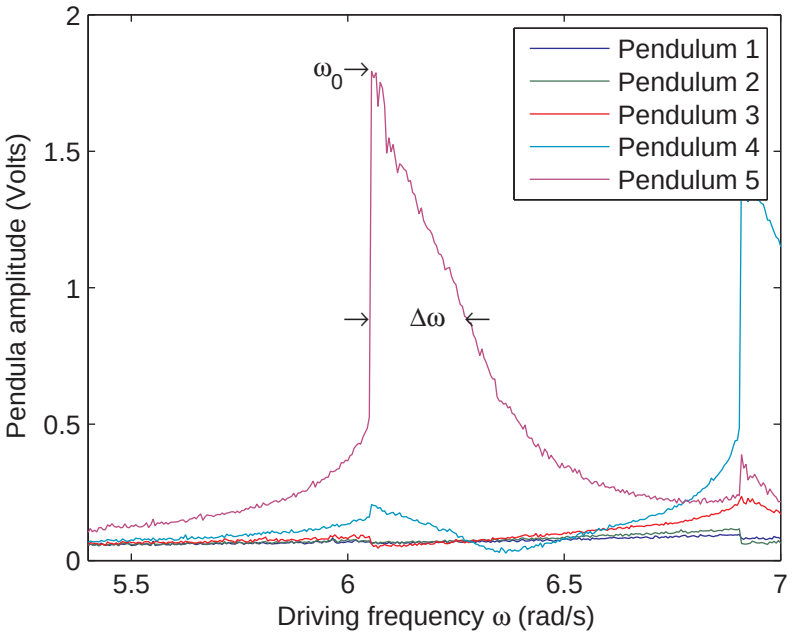

Figure 4.6: $\Delta\omega$ is defined as the width of the amplitude curve at half of its maximum amplitude.

After averaging and taking the worst case scenario, it was found that $\mu \approx 0.1$.

This is a useful estimation, as there exists no analytical formula for multiple coupled oscillators, that relates Q to the damping constant.

4.2 Adjusting the lengths

Now that the model has been analyzed and compared to the experimental set-up, it was found to behave as expected, so predictions can now be made using it. In this section, three different situations will be considered. For convenience, the system will now be considered linear, as then the analytical solution for the amplitudes of each pendulum can be used instead of using the simulation model[3].

4.2.1 Two pendula with equal lengths

For example, what happens when, instead of choosing the pendula to have the lengths as defined in section 4.1, two of those pendula - say, pendula 1 and 5 - have the *same* length?

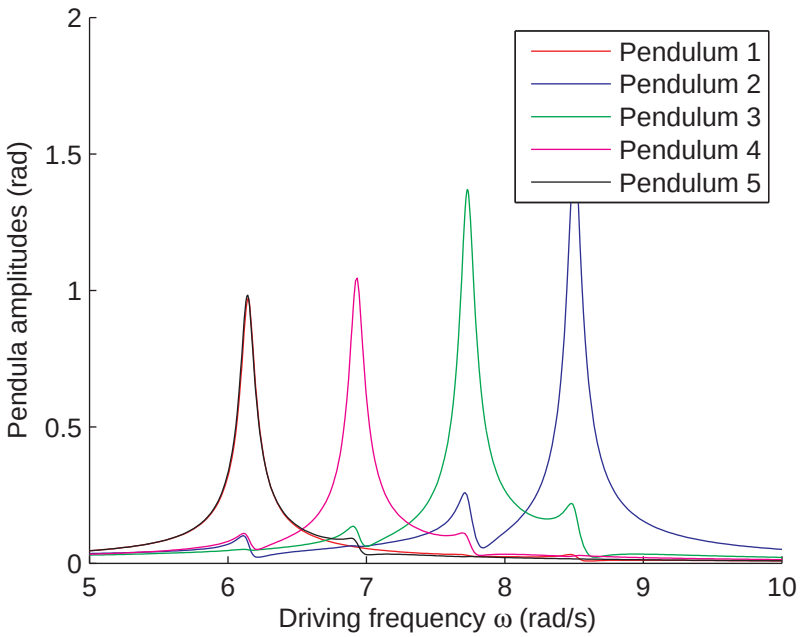

Figure 4.7: Pendula amplitude as a function of the driving frequency in the case that pendula 1 and 5 have identical lengths.

[3]The analytical solution can calculate the amplitude response (not θ_n) much faster than if the simulation model was used. It was already determined in section 4.1.1 that both results are identical, so this method is valid.

In the simulation model, this is easily altered. In this case the following lengths were changed: $l_1 = l_5 = 0.311\ m$, and the other pendula lengths are as previously defined. The result of this calculation is presented in Figure 4.7.

As can clearly be observed, the model predicts that in this case pendula 1 and 5 will both have roughly the same resonance frequencies[4] and they will also have roughly the same amplitudes. Both pendula 1 and 5 will have much larger maximum amplitudes if the driving frequency is chosen to be that of the resonance frequency of these pendula whereas the other pendula will have a relatively small amplitude. This situation was also tested in the experimental set-up and the exact same behaviour was observed, meaning the model adequately predicted this behaviour.

4.2.2 V-shape

Another interesting example is when the pendula lengths are chosen so that the system is symmetric in shape. Take for example a V-shape, where $l_1 = l_5 = 0.155\ m$, $l_2 = l_4 = 0.183\ m$ and $l_3 = 0.205\ m$.

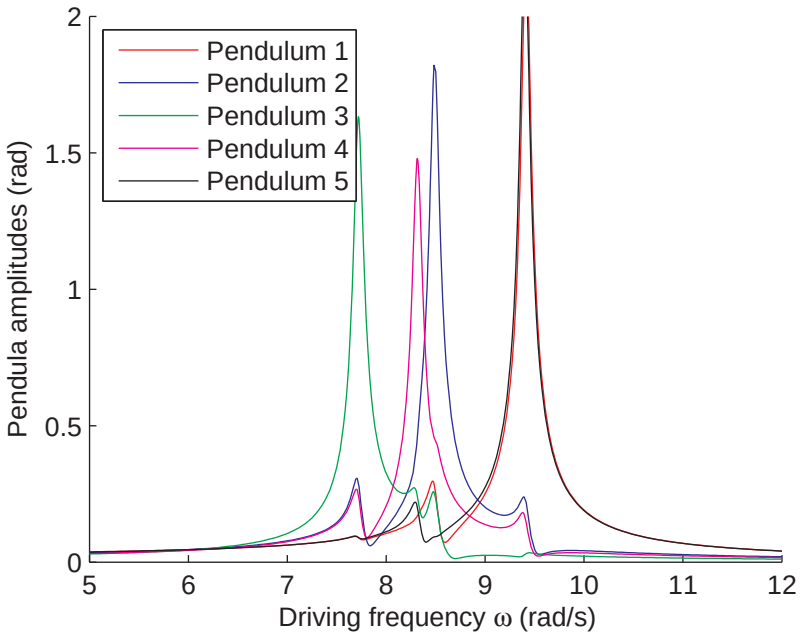

Figure 4.8: Pendula amplitude as a function of the driving frequency in the case of the lengths being chosen in a V shape.

In the ideal case where all parameters are equal for all pendula except for

[4]It is important to note that not all other parameters are equal for both these pendula, so their responses will be slightly different.

the newly defined lengths, the expectation would be that there would only be three resonance frequencies. In the case where the actual real parameters are chosen, the result is as can be seen in Figure 4.8.

As can be seen, pendula 1 and 5 overlap very well, whereas pendula 2 and 4 overlap fairly well. This is obviously due to the non-ideal parameters of both pendula 2 and 4, but not unimportantly also of their neighbouring pendula as neighbouring pendula will greatly influence each other. This behaviour was once again tested against the experimental set-up and the behaviour was as described by the model.

4.2.3 All pendula with equal lengths

The final test will be where all pendula have the same length. As was derived in Chapter 1, in that case there should be only one resonance frequency of the system, and the amplitude responses as a function of the driving frequency should overlap - provided that all parameters are equal per pendulum. In the model, the lengths were chosen to be $l_1 = l_2 = l_3 = l_4 = l_5 = 0.205\ m$. The response is as shown in Figure 4.9.

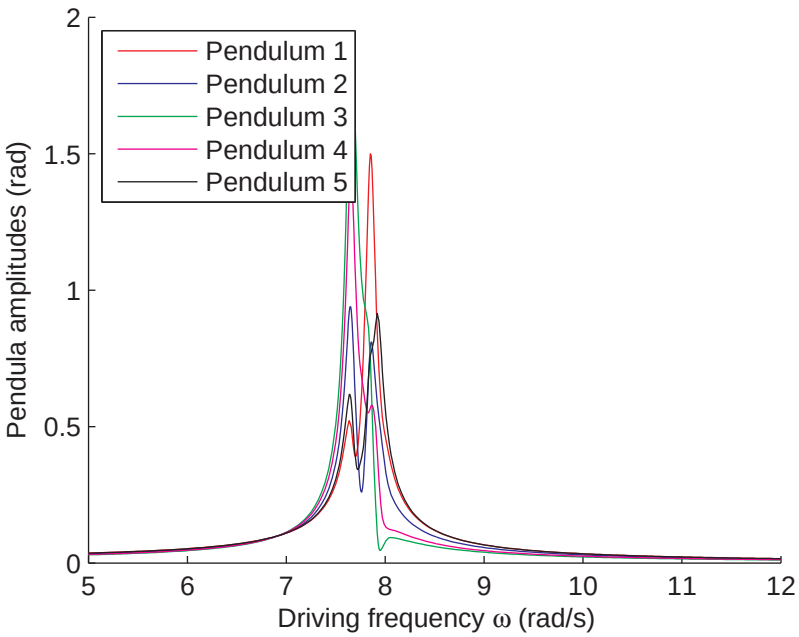

Figure 4.9: Pendula amplitude as a function of the driving frequency in the case of the lengths being chosen equal for all pendula.

This graph shows by far the most interesting result. Where a perfect overlap would be expected in the ideal case, it is obvious that in the experimental case

no such thing will happen. To observe more closely what happens, a close-up is shown in Figure 4.10.

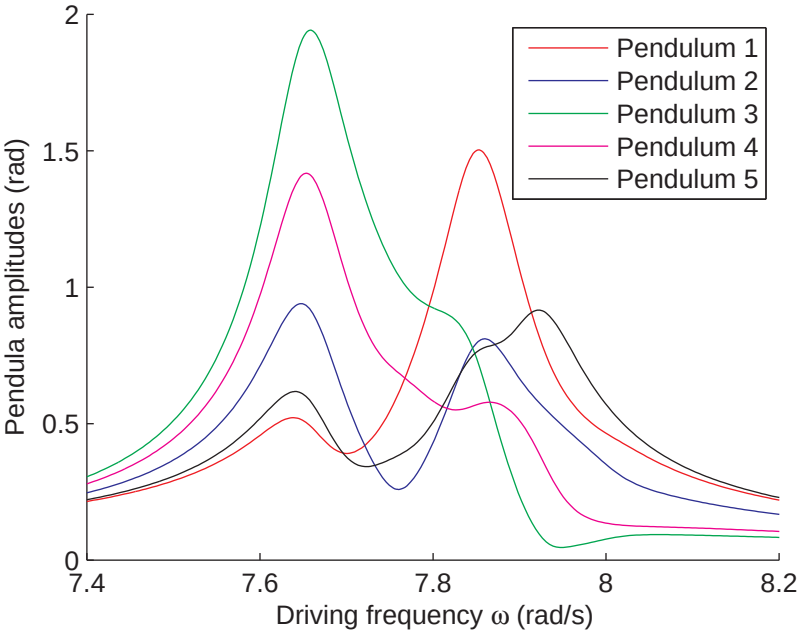

Figure 4.10: Close-up of the response in Figure 4.9.

Clearly the altering parameters have a profound effect on the behaviour of this system. Upon testing, it was clear that setting all masses equal while keeping other parameters as they were originally had no significant effect. However, the same could be said of the pendulum-coupling spring constants, and to a lesser degree of the axle-coupling spring constants. It appears that if only one of these parameters differs slightly from pendulum to pendulum, the system responds strongly in the sense that it will deviate relatively much from the ideal case.

Chapter 5

A driving pulse

In Chapter 2, a theoretical description of the set-up was made, where continuous driving was assumed of the form $\gamma = \gamma_0 cos(\omega t)$. In Chapter 4, the results of the performed simulations were validated. It has been shown that the pendulum set-up has five characteristic resonance frequencies, for five different lengths of the pendula. By choosing one of these characteristic eigenfrequencies and driving the system at this specific frequency with a continuous sinusoidal signal, it was possible to excite one pendulum significantly more than the others.

However, the pendulum set-up was built to explain and investigate the analogy with CARS spectroscopy and coherent control. The point is that in CARS, molecules will always be excited with a certain broadband light pulse - they will be not be continuously excited. The reason for this is that the intensity of the received CARS signals scales with the cube of the intensity of the incoming signal, i.e. $I_{CARS} = \chi I_{IN}^3$, where χ is a proportionality factor. In general, this constant χ is very small, such that the incoming signal has to have a high intensity to be able to measure the CARS signal. A light pulse can have a much higher peak intensity than a continuous light beam while still outputtig the same amount of power. Using a pulse, then, is desirable, otherwise a laser with an output power in the order of MW would be required.

The problem is then translated back in terms of the pendulum model as finding a driving pulse that will excite one pendulum significantly more than other pendula. In this Chapter, an attempt will be made to find and define such a pulse, where Chapters 2 and 4 will be used as guidelines.

5.1 General idea of the shaped pulse

From the CARS perspective, suppose that an incident pulse with a very narrow frequency spectrum, such that it has one specific frequency, strikes a molecule. This frequency can be chosen such that it matches the resonance frequency of one specific bond in a molecule, therefore exciting this specific bond. However, energy will immediately leak to other bonds due to coupling between adjacent

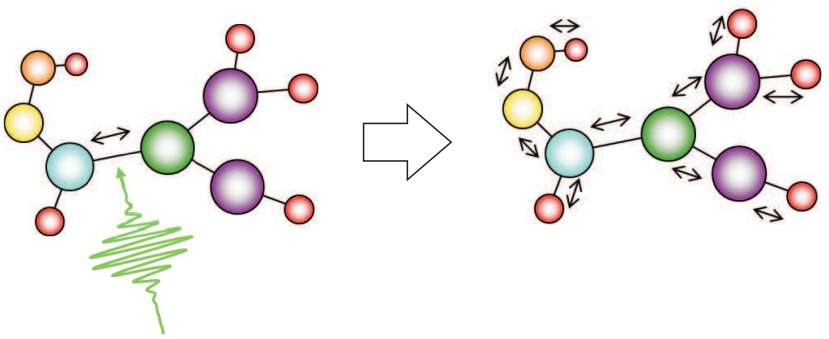

Figure 5.1: Exciting a molecule with a pulse [5].

atoms, resulting in them being indirectly excited as well. See Figure 5.1 for a schematic drawing.

The idea is then to take an incident pulse with a broader frequency spectrum, that contains the frequencies of all bonds in the molecule with the right amplitudes and phases for destructive interference, such that one specific bond will be excited significantly more than others. See Figure 5.2 for another schematic drawing of this situation.

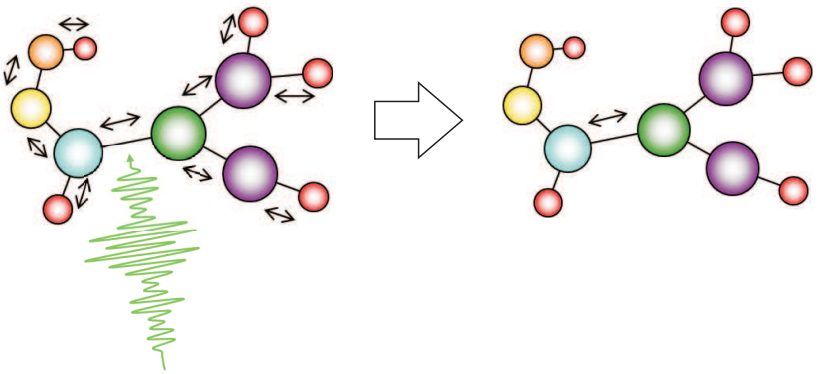

Figure 5.2: Exciting the same molecule, but now with a shaped pulse [5].

This (broader) amplitude spectrum will be defined by a Gaussian centered around a resonance frequency of a bond that should be excited (so for the pendulum model at a resonance frequency of one specific pendulum). The width of the Gaussian should be chosen such that it contains all of the systems resonance frequencies, because specifically these frequencies could contribute to the destructive interference of other bonds. Together with a properly chosen phase spectrum, this input signal can excite the bonds in the molecule in the right way so as to ensure that only one bond will be excited significantly more than others - if only for a brief moment in time. This raises the question of what the

phase spectrum should look like. The next section will elaborate on this.

5.1.1 Flipping the phase of the driving signal

In Chapter 2, it was shown how $\Theta_n(\omega)$ was derived. This formula is called the frequency response or transfer function, because it describes how the system responds to different frequencies. When applying a driving signal $\gamma(t)$, the response of a pendulum in the frequency domain, $\tilde{\Theta}_n(\omega)$, is given by the product of the transfer function and the Fourier transform of $\gamma(t)$

$$\begin{aligned} \tilde{\Theta}_n(\omega) &= \Theta_n(\omega)\hat{\gamma}(\omega) \\ &= |\Theta_n(\omega)|e^{i\varphi_n(\omega)}|\hat{\gamma}(\omega)|e^{i\varphi_d(\omega)} \\ &= |\Theta_n(\omega)||\gamma(\omega)|e^{i(\varphi_n+\varphi_d)} \end{aligned} \tag{5.1}$$

Now suppose that $\hat{\gamma}(\omega)$ has a frequency spectrum that is relatively wide compared to the transfer functions $\Theta_n(\omega)$ and envelopes these transfer functions at the same time, as shown in Figure 5.3. Because the fourier transform of a Gaussian is once again a Gaussian, this shape will be chosen for $\hat{\gamma}(\omega)$ for convenience. The larger the width of the Gaussian envelope, the more it will approach the Fourier Transform of a delta pulse, which is $\Im\{\delta(t)\} = 1$. Thus, if the width is chosen large enough, (5.1) simplifies to

$$\boxed{\tilde{\Theta}_n(\omega) \approx |\Theta_n(\omega)|e^{i(\varphi_n+\varphi_d)}} \tag{5.2}$$

Equation (5.2) is an important result as it states that all of the frequency components that $\tilde{\Theta}_n(\omega)$ contains, might be given an identical phase. Setting the phase of the driving signal φ_d opposite to φ_n would do the job

$$\varphi_d = -\varphi_n$$

The phase of a pendulum φ_n changes as shown in Figure 5.3.

The phase of the driving signal should then be chosen equal to the light-blue dashed line. The polar plot in Figure 5.4 illustrates this idea: if ω increases, the blue circle will be traced in the direction of increasing numbers. Its corresponding phase φ_n, then runs from 0 to π. Now suppose the driving function traces the green circle in the opposite direction as again indicated by the increasing numbers. Its corresponding phase φ_d then runs from 0 to $-\pi$. It is obvious from (5.1), that their phases will add up to yield $\tilde{\Theta}_n$. The effect is then that the net response lies across the positive real axis, because all vectors will add up across these axis. Note that this would not be case when using a flat phase, $\varphi_d = 0$, as then horizontal vector components would cancel out, resulting in a net vertical vector, which at the same time is obviously less in magnitude than would be the case if the phase of the drive signal is flipped.

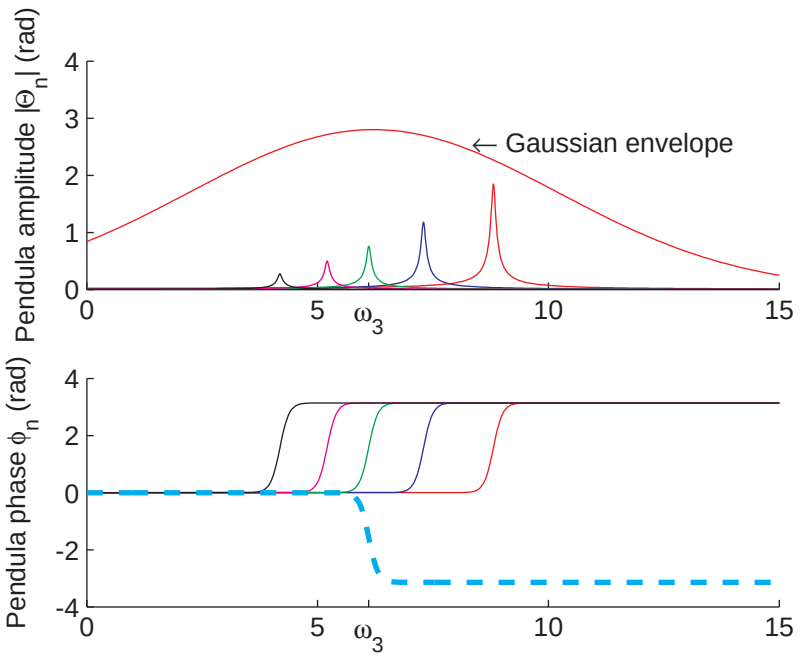

Figure 5.3: The amplitude and phase response for a system of five uncoupled pendula. The Gaussian envelope which is multiplied with in the frequency domain is shown as well. The blue dashed line represents the phase of this envelope, and has the opposite phase of pendulum 3.

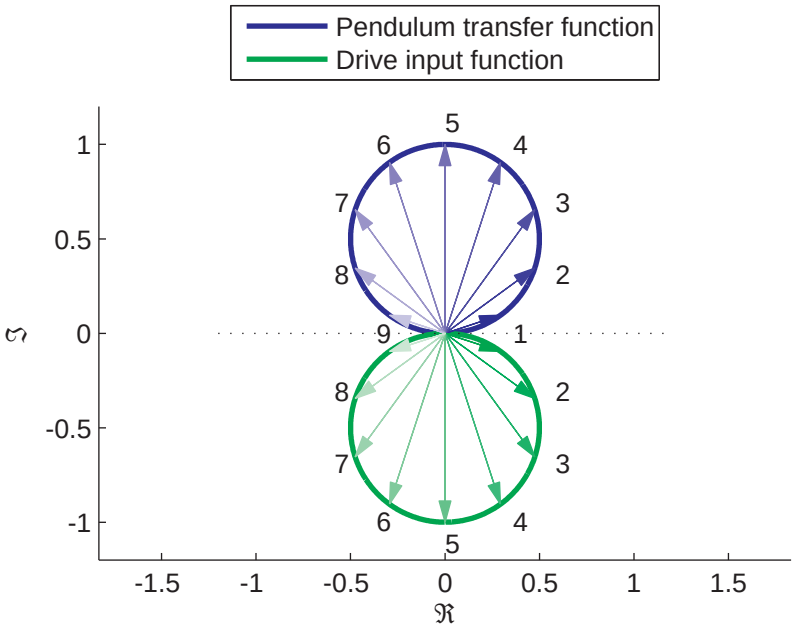

Figure 5.4: Polar plot of the pendulum transfer function and the drive input function.

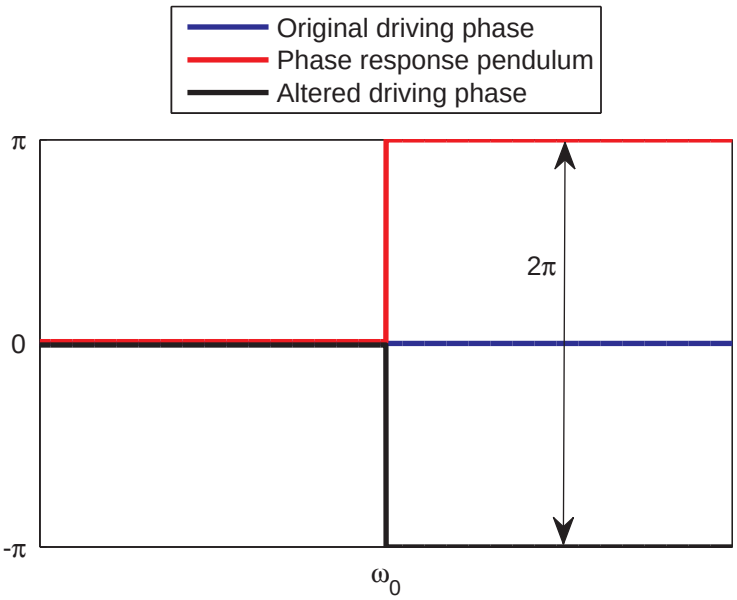

Figure 5.5: Changing the drivers phase by π at resonance frequency ω_0, will bring the driver and pendulum back in phase again.

In the remaining part of this Chapter, derivations will be made using the ideal phase response of the system for convenience, as the phase response does not differ too much from the ideal case as long as μ is not too large - which it was previously determined not to be. Beside this, the driving axle of the pendulum model will probably not be able to follow the exact phase response due to its own resolution limitations.

In this ideal case, the phase jumps previously shown in Figure 5.3 will now assume the form of Figure 5.5. This phase jump is chosen to occur when the driving frequency equals ω_0, the resonance frequency of the pendulum that is to be excited. Only this pendulum will be affected by this phase flip, since all other pendula have amplitudes that are negligible at these frequencies, and a phase flip there will go unnoticed. The effect of this phase flip is similar to what was previously described for the non-linear case, although in this case, without the phase flip in the drive signal, the amplitude components of the pendulum would add up to a total of zero at $t = 0$, whereas all amplitude components will add up constructively if the phase flip *is* introduced. Therefore, this method should theoretically produce a much better response of the pendulum that is to be excited than before.

Coupling the pendula will introduce changes in the phase spectra of the pendula, see Figure 5.6. The sharps peaks in the phase spectrum are due to neighbouring pendula that are resonating. Thus driving the coupled system

with a pulse with has the same shaped phase, cannot be expected to work as well in the uncoupled case, but still it is expected to work better than if no phase flip would be used.

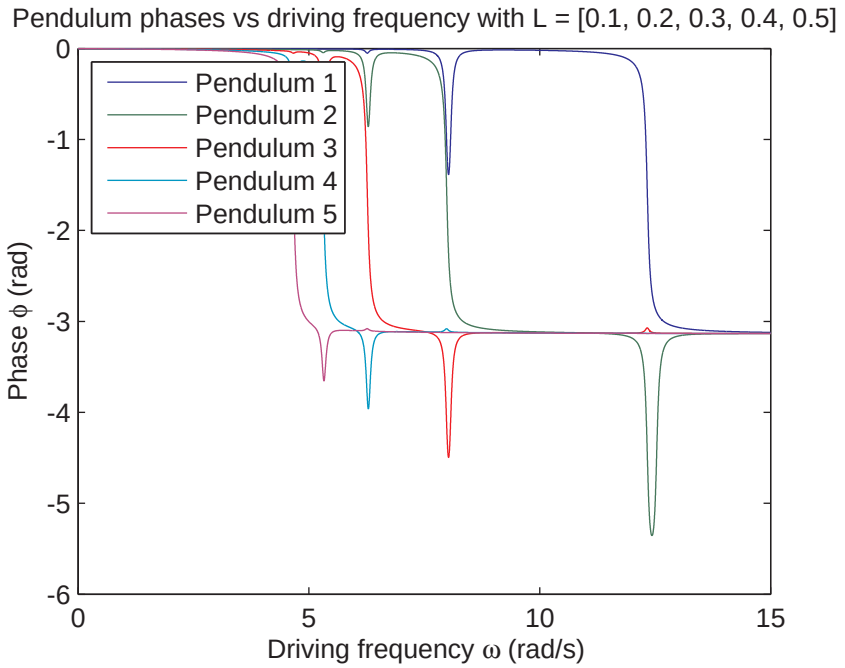

Figure 5.6: Phase behaviour of pendula in the coupled system, when using lineair approximation.

In section 5.1.2, the shape of the actual pulse will be determined when its phase spectrum is flat, i.e. $\varphi(\omega) = 0$, followed by a numerically inverse Fourier transformed pulse in section 5.1.4, with the altered phase spectrum shown in Figure 5.5. These pulses will then be implemented as driving signals in the simulations, such that the behavior of both pulses can be investigated.

5.1.2 Defining the (angular) frequency spectrum of the pulse

From Fourier analysis it is known that

$$\mathcal{F}\left\{e^{-\xi t^2}(t)\right\} = \sqrt{\frac{\pi}{\xi}} e^{-\frac{\omega^2}{4\xi}} \qquad \xi \in \mathbb{R}, \xi > 0 \tag{5.3}$$

In this case, only a symmetric amplitude spectrum makes sense, because the corresponding time signal has to be real valued. Centering the Gaussian from

(5.3) in frequency domain around $+\nu$, setting $\xi = \frac{1}{2}\sigma^2$, multiplying by an arbitrary constant α and adding a similar mirrored (in $\omega = 0$) Gaussian to preserve symmetry, the new amplitude spectrum is then defined as

$$A(\omega) = \alpha \frac{\sqrt{2\pi}}{\sigma} \left[e^{-\frac{(\omega+\nu)^2}{2\sigma^2}} + e^{-\frac{(\omega-\nu)^2}{2\sigma^2}} \right] \tag{5.4}$$

Note that the value of σ determines the width of the Gaussians, which has to be chosen such that all of the system's eigenfrequencies are present in the amplitude spectrum, as explained in the previous section. Furthermore, ν will be chosen equal to the resonance frequency of a pendula. The corresponding phase spectrum will only make sense when it is odd, because as was mentioned before, the time signal has to be real valued. It is initially defined as

$$\varphi_d(\omega) = 0$$

Such that the frequncy spectrum of the time signal is defined as

$$\hat{\gamma}(\omega) = A(\omega) e^{i\varphi_d(\omega)}$$

The signal in the time domain follows from the inverse Fourier transform

$$\begin{aligned} \gamma(t) &= \frac{1}{2\pi} \int_{-\infty}^{\infty} \hat{\gamma}(\omega) e^{i\omega t} d\omega \\ &= \alpha e^{-\frac{1}{2}\sigma^2 t^2} (e^{-i\nu t} + e^{i\nu t}) \\ &= 2\alpha e^{-\frac{1}{2}\sigma^2 t^2} cos(\nu t) \end{aligned} \tag{5.5}$$

Apparently, $\gamma(t)$ is a sinusoid with a Gaussian envelope. A plot of the amplitude- and phase spectrum of $\gamma(t)$, as well as $\gamma(t)$ itself with its Gaussian envelope is shown in Figure 5.7. For convenience, the constants have been set to $\alpha = 1$; $\sigma = 1$; $\nu = 5$.

5.1.3 Using MATLAB for the inverse Fourier transform

In the previous subsection, $\gamma(t)$ has been derived analytically. This becomes a lot harder, if not impossible, when the phase spectrum will be changed. It was therefore decided to use the Inverse Fast Fourier Transform function of MATLAB, to transform the signal from frequency domain to time domain. Performing an inverse Fourier transform using MATLAB on the amplitude and phase spectrum, shown in Figure 5.7, should yield the same result as the analytical result of (5.5). However, they will not match in general. This is due to periodicity in the time domain assumed by the IFFT function, but the amplitude spectrum defined by (5.4) transforms into $\gamma(t)$, and is clearly non periodic. This problem can be resolved quite easily: when calculating the inverse Fourier transform, it should be calculated over a sufficiently long time interval. Comparing the analytical with the numerical inverse Fourier transform has shown that a time

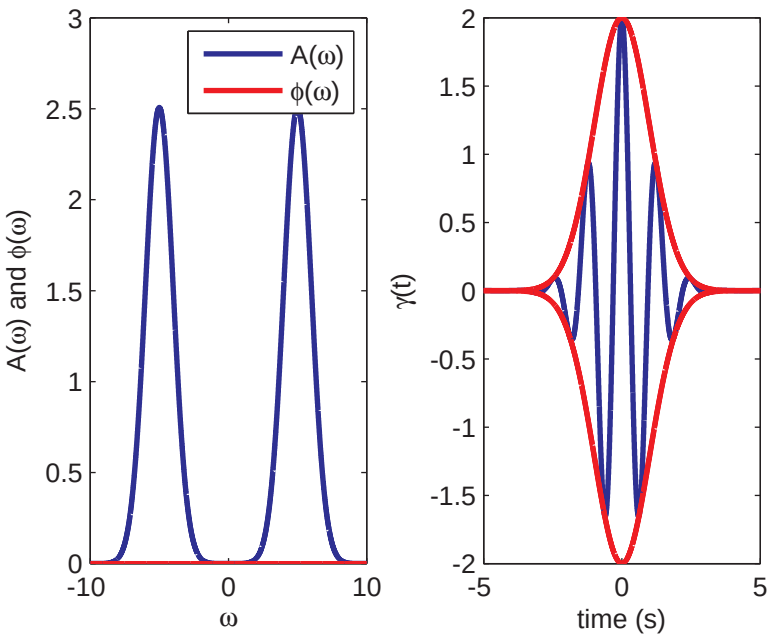

Figure 5.7: On the left: amplitude and phase spectrum of $\gamma(t)$; On the right: $\gamma(t)$ with the gaussian envelope.

interval from $\widetilde{T} = [-100 \quad 100]$ is more than sufficient, because both signals could hardly be distinguished anymore. Effectively, MATLAB now sees a time signal which is apparently long enough to treat it as 'non-periodic'. Another consequence of MATLAB assuming periodicity is that the amplitude spectrum will scale with the length of the time interval, thus $A(\omega) \sim 1/\widetilde{T}$.

When performing an inverse Fourier transform, it is imperative that the sampling frequency ω_s is high enough, in order to be able to follow high frequency components. The minimum sample rate required to completely reconstruct the time signal is the Nyquist frequency $\omega_s = 2\omega_b$, where ω_b is the bandwidth of the frequency spectrum. From (5.4) it follows that a sampling frequency $\omega_s \gg \nu + 4\sigma$ will be more than sufficient. From the sample frequency, the corresponding time step then follows as $dt = \frac{2\pi}{\omega_s}$.

The aforementioned describes the main issues and most important basics of the algoritm that carries out the inverse Fourier transform. See also Appendix B.

5.1.4 Re-defining the phase spectrum

The phase spectrum of $\gamma(t)$ will now be re-defined as explained in section 5.1, such that the driver will be in phase with the pendulum for all of the frequencies that the driving signal contains. This phase spectrum is show in Figure 5.8, and

can mathematically be represented in terms of the Heaviside function $\mathcal{H}$

$$\varphi_s(\omega) = \pi \left[\mathcal{H}(\omega - \omega_0) - \mathcal{H}(-\omega - \omega_0)\right]$$

Changing the phase spectrum of $\gamma(t)$ will not change the energy content of the phase altered signal $\gamma_s(t)$, because their amplitude spectrum is the same

$$E_f = \frac{1}{2\pi} \int_{\infty}^{\infty} |\hat{\gamma}(\omega)|^2 \, d\omega = \frac{1}{2\pi} \int_{\infty}^{\infty} A^2(\omega) d\omega = \frac{1}{2\pi} \int_{\infty}^{\infty} |\hat{\gamma}_s(\omega)|^2 \, d\omega$$

From this, one would conclude that the response of the system to the original pulse and phase altered pulse may be compared, since both signals put the same amount of energy into the system. However, a problem arises as $\gamma_s(t)$ will not converge to zero as $t \to \pm\infty$ whereas $\gamma(t)$ converges to zero quickly and is at only one percent of its maximum when $\frac{1}{2}\sigma^2 t^2 > 4$. Obviously, one would want to drive the system with a pulse of a defined and finite duration. The difference between $\gamma(t)$ and $\gamma_s(t)$ can be qualitatively understood in terms of the frequency spectrum. A flat phase spectrum, shown in Figure 5.7, results in $\gamma(t)$ being built up of cosines of different frequencies, centered around $t = 0$. Because they have different frequencies, the cosines will go out of phase as $|t| > 0$, resulting in destructive interference - hence the signal converges to zero for large $|t|$. If the flat phase spectrum is now altered to the one shown in Figure 5.8, again cosines of different frequencies will add up. However, now not all of them will be centered around $t = 0$, therefore destroying the symmetry that $\gamma(t)$ has. This in turn then partially destroys the (complete) destructive interference and the signal will not converge to zero anymore.

To obtain a phase altered pulse with a finite duration, it was decided to cut off $\gamma_s(t)$, which defines a new signal $\gamma_s'(t)$. The typical cut off time, designated t_c, has been made dependent on the typical width of the original pulse. The typical width of the pulse has been defined as the time at which $\frac{1}{2}\sigma^2 t^2 = 8$, to be on the safe side (the amplitude of the pulse will then be negligible, as it will be in the order of 10^{-4} radians), or $t_{typicalwidth} = \frac{4}{\sigma}$. In general, this value of t will not be a root of γ_s, and it would be better to avoid t_c to be such that$\gamma_s(t_c) \neq 0$ for practical reasons: the motor of the demo model always starts with zero amplitude and defining a pulse which starts with a finite amplitude is therefore not feasible in practice. If one would just ignore this, the actual applied pulse would be slightly different.

An algorithm has been written that searches for the closest zero around $t_{typicalwidth}$, see *pendulum_inverse_fourier.m*, added to Appendix B. This newly found time value is then assigned t_c. Note that because of symmetry, once a root is known to be located at $t = t_c$, another zero is automatically located at $-t_c$. Even though both pulses are now well defined on $[-t_c \quad t_c]$, cutting off $\gamma_s(t)$ throws away a part of its energy content.

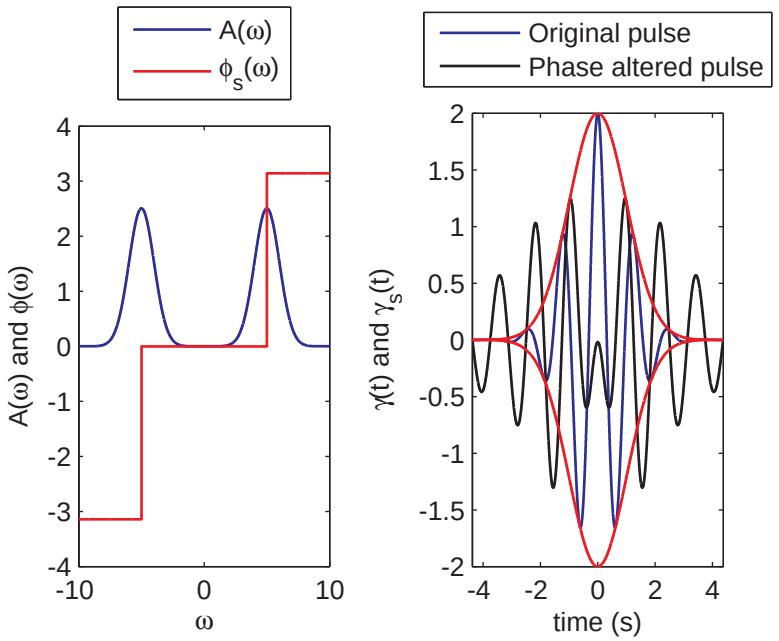

Figure 5.8: On the left: amplitude and altered phase spectrum of $\gamma_s(t)$; On the right: the original pulse $\gamma(t)$ and the phase altered pulse $\gamma_s(t)$.

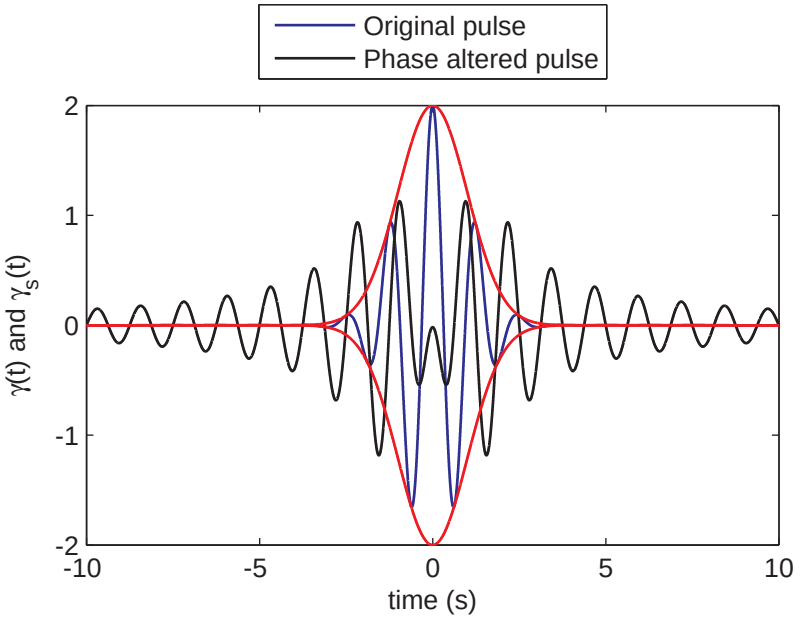

Figure 5.9: $\gamma(t)$ and $\gamma_s(t)$ on a extended time domain.

Therefore $\gamma_s'(t)$ has to be rescaled in order to have the same energy content as $\gamma(t)$. This scaling factor is determined numerically by the algorithm and follows as

$$scalingfactor = \sqrt{\frac{E_{\gamma(t)}}{E_{\gamma_s'(t)}}} = \sqrt{\frac{\int_{-t_c}^{t_c} |\gamma(t)|^2 \, dt}{\int_{-t_c}^{t_c} |\gamma_s'(t)|^2 \, dt}}$$

Multiplying $\gamma_s'(t)$ by this scalefactor then gives both signals the same energy content. An example of the result can be seen in Figure 5.8 and on an extended domain in Figure 5.9.

The system's behavior to $\gamma(t)$ and $\gamma_s'(t)$ to the uncoupled as well as the coupled system will be tested in the next section.

5.2 Response of the system to both kind of pulses

In this section the response of the system to both kinds of pulses - the one with and without phase flip - will be tested. The results will be easier to analyze when the lengths of the pendula are not closely spaced, because then the transfer functions would overlap. Therefore, the lengths are chosen to lie 0.1 m apart, such that $l_1 = 0.1$; $l_2 = 0.2$; $l_3 = 0.3$; $l_4 = 0.4$; $l_5 = 0.5$. Furthermore, the coupling spring constants and masses will all be chosen identical. First, simulations will be performed with the uncoupled system, where different values for σ will be taken. The reason for this is that it is already known how the system will response when σ is taken very small, because the time signal is then approximately that of a continuous sinusoidal shape, which can be used as a check. Secondly, the response of the coupled system to both pulses will be simulated and this time only for a large value of σ.

5.2.1 Uncoupled system, small σ

The center frequency of the Gaussian, ν, will be set to the resonance frequency of pendulum 1, so the phase flip will also occur at this frequency. Initially a small value for σ will be chosen, so that the frequency spectrum is small and the signal in the time domain is sinusoidally shaped with a large envelope. For the case *without* a phase flip, the response of the system is shown in Figure 5.10. With phase flip, the system responds as shown in Figure 5.11.

As can been seen in 5.10, all pendula respond to the pulse, and pendulum 1 does indeed have a significantly larger amplitude than the others. Because the system was excited with the characteristic frequency of pendulum 1, it will keep oscillating for a while until its damped out.

Observing the case with phase flip, shows that the response of pendulum 1 is now stronger: a relatively high amplitude is now present in a larger time domain. The response of the other pendula has decreased slightly, but this is mainly caused by γ_s, which becomes smaller in maximum amplitude after the phase shift. The same phase shift gives a longer (nonzero) signal in the

time domain as explained in the previous section. Therefore, the pendula will oscillate in a longer time domain, which can be observed as well.

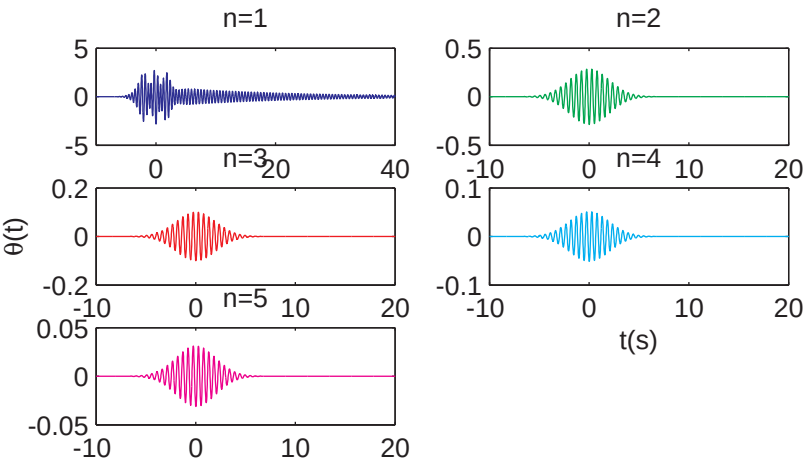

Figure 5.10: Response of the system, when no phase flip is applied.

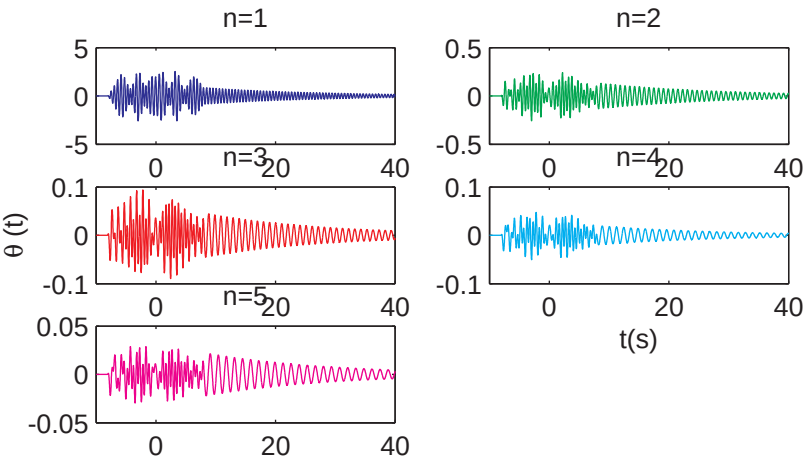

Figure 5.11: Response of the system, when a phase flip is applied.

5.2.2 Uncoupled system, large σ

The range of eigenfrequencies of the pendula lies between 4.6 rad/s and 12.1 rad/s. Setting $\sigma = 4$ will then be large enough for the Gaussian envelope to contain all of the resonance frequencies. This wide frequency spectrum will in turn yield a very narrow pulse in the time domain. The response of the system for the case without and with phase flip are again plotted. See Figures 5.12 and 5.13.

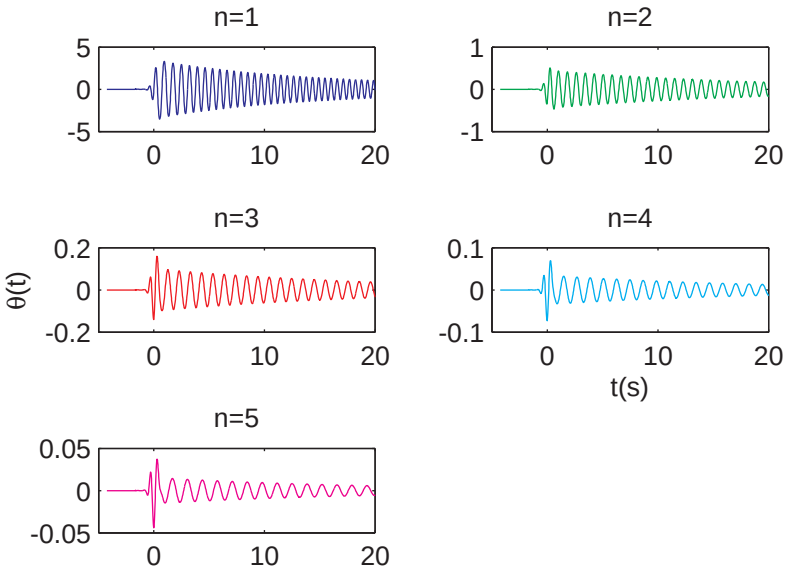

Figure 5.12: Response of the system, when no phase flip is applied.

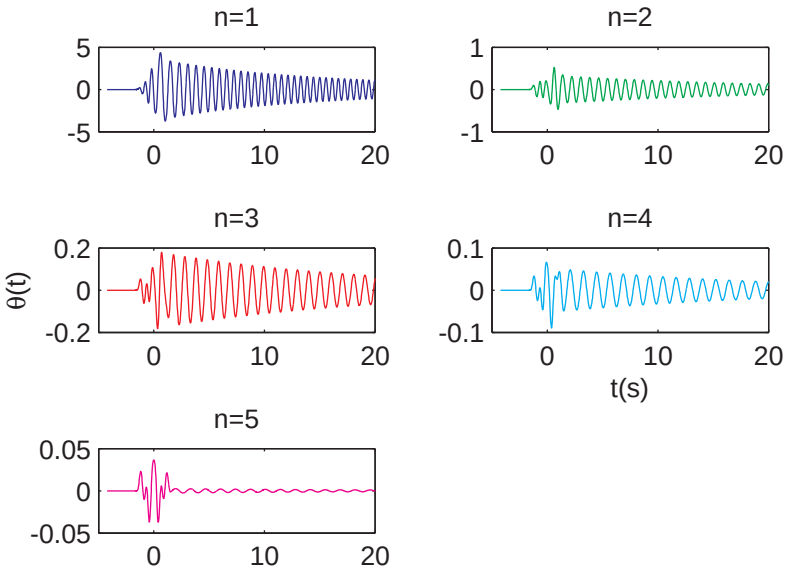

Figure 5.13: Response of the system, when a phase flip is applied.

Because the frequency spectrum is now wider, it also contains the characteristic frequencies needed to excite other pendula. Therefore, they will oscillate a said period of time, until they are damped out. Note the difference between Figure 5.10 and 5.12, where only pendulum 1 oscillates over a longer time than the other pendula.

If the phase flip is now applied, the system responds as shown in Figure 5.13. Note that pendulum 1 now has a higher peak just after $t = 0$, which was not present in the case of no phase flip.

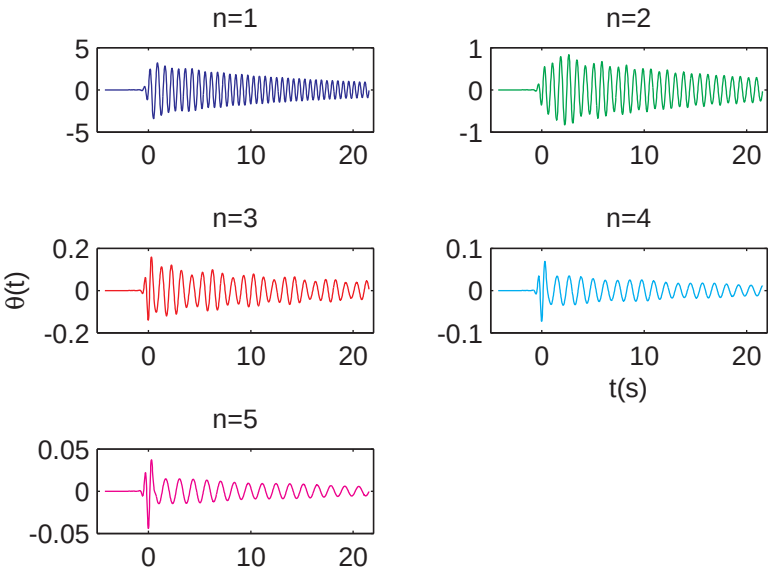

Figure 5.14: Response of the coupled system to the pulse, when no phase flip is applied.

5.2.3 Coupled system

When the system is coupled, the responses to both pulses are as shown in Figure 5.14 and 5.15. From the figures, it can be deduced that the maximum amplitude of pendulum 1 has increased about 5 percent. However, at the same time the amplitude of pendulum 2 has increased as well due coupling between these two pendula. The other pendula also experience a neglible increase in amplitude, probably caused by coupling as well, so pendulum 1 is effective stimulated the most. Therefore, flipping the phase seems to work, even in the coupled case, although the idea of the phase flip was based on the uncoupled case. But, of course, this could be expected, as the phase spectrum of the uncoupled and coupled case have many similarities.

5.2.4 Experimental Setup

For a final comparison, a program in LabView was built, so that the system could be driven with both pulse types. Simulations have shown that the difference in reponse to both pulses is small. In combination with the fact that the driving axle is not able to output the predefined amplitude, as mentioned in Chapter 4, this unfortunately resulted in differences that could not be measured. Therefore the experimental results are not included.

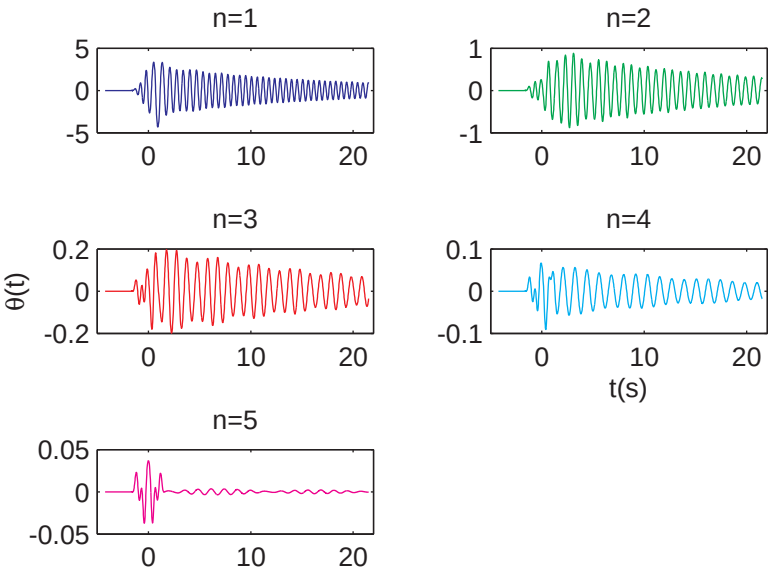

Figure 5.15: Response of the coupled system to the pulse, when a phase flip is applied.

Chapter 6

Conclusion, discussion and recommendations

The coherent control model has been theoretically described and various important parameters in the system have been included. It has been shown that in the configuration where all pendula were given the same length, none of the systems eigenmodes can be stimulated when the system is driven.

Furthermore, a simulation model of the pendulum set-up has been built and was experimentally verified. The simulation model was found to be able to predict the behaviour of the pendulum set-up quite well.

Simulations performed in Chapter 5 have shown that using a phase shaped pulse results in a slightly increased amplitude response of the involved pendulum. Even though the phase shaping analysis was done for an uncoupled system, simulations have shown that it also works for the coupled system - albeit to a lesser extent.

Discussion and recommendations

Currently, the coherent control model is being controlled by the *Evolutionary Smart Learning Algorithm*. A first initial guess for the driving signal is being made by taking a cosine with a Gaussian envelope. Its center frequency in the frequency domain is taken equal to the eigenfrequency of the pendulum - the one to be excited. However, from the analysis in Chapter 2 it can be concluded that the coherent control model has five different eigenfrequencies (when using five different lengths), at which one pendulum is excited significantly more than the others. For a coupled system, the system's eigenfrequencies are not equal to the eigenfrequencies of the pendula. It would therefore be a better initial guess to start with the center frequency equal to an eigenfrequency of the system.

One of the reasons why the experimentally determined amplitude response as a function of the driving frequency did not match the analytically determined one, is because the maximum drive axle amplitude decreased as the driving fre-

quency was increased. For a good comparison it is imperitive that the maximum drive axle amplitude remains constant for all drive frequencies. Furthermore, the motion of the drive axle is overall not very smooth. The amount of noise in the drive signal - although negligible for large driving amplitudes - is an undesired factor when performing real measurements. It was also noticed that the maximum driving amplitude at a fixed driving frequency is not constant. It is therefore recommended that further investigation is performed to find out what is causing this behaviour in the drive axle.

Both the axle coupling springs and the pendula coupling springs were self made, causing their spring constants to differ. The axle-coupling springs differ by a maximum of 30 percent, whereas the pendula-coupling springs differ by as much as 60 percent. When the objective is to use the model to explain CARS to a random person, this will not make much of a difference. However, these differences can no longer simply be neglected when performing (even simple) experiments on the coherent control model, which turns out to be very disturbing. If more detailed experiments are to be performed using the pendulum set-up, it is therefore advised to order new factory produced springs that will result in a less complex system.

The determination of the damping constant in the model was done by averaging the Q-factors of all the different pendula and determining μ from those factors. In reality, each pendula has its own value for μ. For future simulations, the implementation of these different μ values in the simulation model could therefore be considered and the effect on the system could be analyzed.

Nomenclature

l_n	length of the n-th pendulum	m
m_n	mass of the n-th pendulum	kg
γ	driving amplitude as a function of time	$radians$
κ	axle-coupling spring constant	$N \cdot m \cdot radians^{-1}$
$\widetilde{\kappa}$	pendulum-coupling spring constant	$N \cdot m \cdot radians^{-1}$
θ_n	pendulum amplitude as a function of time	$radians$
T_n	kinetic energy of the n-th pendulum	J
U_n	potential energy of the n-th pendulum	J
g	gravitational acceleration	$m \cdot s^{-2}$
y	position relative to the drive axle (negative downward)	m
L_n	lagrangian for the n-th pendulum	J
Θ_n	maximum amplitude of the n-th pendulum	$radians$
ω	driving frequency	$radians \cdot s^{-1}$
ω_s	sampling frequency	$radians \cdot s^{-1}$
ω_b	bandwidth driving signal	$radians \cdot s^{-1}$
ω_r	resonance frequency	$radians \cdot s^{-1}$
t	time	s
γ_0	maximum driving amplitude	$radians$
γ	driving function	$radians$
γ_s	phase altered driving function	$radians$
γ_s'	cut off driving signal	$radians$
t_c	cut off time	s
φ_n	phase response of pendulum n	$radians$
φ_d	phase spectrum of the driving signal	$radians$
φ_s	altered phase spectrum driving signal	$radians$
$\mathbf{M}$	transformation matrix	$-$
Q	quality factor	$-$
η_r	eigenmode	$-$
μ	damping constant	$Ns \cdot m^{-1}$
τ	torque	$N \cdot m$
σ	width of Gaussian in frequency domain	$radians \cdot s^{-1}$
ν	offset frequency Gaussian in frequency domain	$radians \cdot s^{-1}$
α	amplitude factor Gaussian in frequency domain	$-$
E	energy content	$radians^2 \cdot s$

Acknowledgements

During our time at the Optical Sciences group at the University of Twente, we have been given the opportunity to experience what it is like to be part of a team of researchers and it has left us with fond memories. We would therefore like to thank all the members of the Optical Sciences group for their warm welcome, great humor and enthousiasm during the past weeks. We really enjoyed ourselves and felt accepted right from the start.

In particular, we would like to thank Jennifer Herek and Herman Offerhaus for giving us the opportunity to take on this assignment and for the assistance they provided us with. Our work could also not have been possible without the help of Jeroen Korterik. Thanks to his expert knowledge of Labview, no matter what kind of program we asked for, it was always made in the shortest amount of time and worked just as expected.

We hope that our contributions to the coherent control will be of use in the future and that it may spark more interest in this phenomenon - it sure caught our attention!

Bibliography

[1] David C. Lay, *"Linear Algebra and Its Applications"*. Third International edition, February 2006.

[2] G. Hemink and Erik Dietrich, "*Making a coherent control model*". Bachelor thesis, University of Twente, October 2008.

[3] T.Thornton and B.Marion, *"Classical Dynamics of Particles and Systems"*. Fifth Edition, 2004.

[4] Encyclopedia of Laser Physics and Technology, Rüdiger Paschotta, "*Q factor*". RP Photonics Consulting, April 2011.

[5] E.Dollekamp and J.Sueters, *Poster on "A Coherent Control Demo Model"*. University of Twente, September 2010.

[6] A.A. Stoorvogel, "*Signals and Transforms*", Lecture Notes, University of Twente, July 2008.

Appendix A

MATLAB Files Chapter 3

measurements_analytical.m

```
% Calculate the amplitude response of the system analytically - this method
% is much faster than using the simulation model itself to determine the
% amplitude response as a function of the driving frequency.
maple restart;
format long

% Generic constants
g = 9.81;

% Masses of the pendula
m1 = .235;
m2 = .240;
m3 = .25;
m4 = .255;
m5 = .22;

% Lengths of the pendula
l1=.1;
l2=.15;
l3=.2;
l4=.25;
l5=.3;

% Spring constants of the axle springs
kappaas1 = .13;
kappaas2 = .12;
kappaas3 = .101;
kappaas4 = .112;
kappaas5 = .121;

% Spring constants of the coupling springs
kappaover1 = 0.012;
kappaover2 = 0.016;
```

```
kappaover3 = 0.010;
kappaover4 = 0.011;

% Special constants
a1 = kappaas1/(m1*l1^2);
a2 = kappaas2/(m2*l2^2);
a3 = kappaas3/(m3*l3^2);
a4 = kappaas4/(m4*l4^2);
a5 = kappaas5/(m5*l5^2);

b1 = kappaover1/(m1*l1^2);
b2 = kappaover1/(m2*l2^2);
b3 = kappaover2/(m2*l2^2);
b4 = kappaover2/(m3*l3^2);
b5 = kappaover3/(m3*l3^2);
b6 = kappaover3/(m4*l4^2);
b7 = kappaover4/(m4*l4^2);
b8 = kappaover4/(m5*l5^2);

mu = 0.1;
gamma1 = 0.1;

% DEFINING THE MATRIX
syms t
A = [-t^2+g/l1+a1+b1+j*t*mu, -b1, 0, 0, 0;...
     -b2, -t^2+g/l2+a2+b2+b3+j*t*mu, -b3, 0, 0;...
     0, -b4, -t^2+g/l3+a3+b4+b5+j*t*mu, -b5, 0;...
     0, 0, -b6, -t^2+g/l4+a4+b6+b7+j*t*mu, -b7;...
     0, 0, 0, -b8, -t^2+g/l5+a5+b8+j*t*mu];

% PENDULUM 1
B = [a1*gamma1, -b1, 0, 0, 0;...
     a2*gamma1, -t^2+g/l2+a2+b2+b3+j*t*mu, -b3, 0, 0;...
     a3*gamma1, -b4, -t^2+g/l3+a3+b4+b5+j*t*mu, -b5, 0;...
     a4*gamma1, 0, -b6, -t^2+g/l4+a4+b6+b7+j*t*mu, -b7;...
     a5*gamma1, 0, 0, -b8, -t^2+g/l5+a5+b8+j*t*mu];
amp1=simplify(det(B)/det(A));

% PENDULUM 2
C = [-t^2+g/l1+a1+b1+j*t*mu, a1*gamma1, 0, 0, 0;...
     -b2, a2*gamma1, -b3, 0, 0;...
     0, a3*gamma1, -t^2+g/l3+a3+b4+b5+j*t*mu, -b5, 0;...
     0, a4*gamma1, -b6, -t^2+g/l4+a4+b6+b7+j*t*mu, -b7;...
     0, a5*gamma1, 0, -b8, -t^2+g/l5+a5+b5+j*t*mu];
amp2=simplify(det(C)/det(A));

% PENDULUM 3
D = [-t^2+g/l1+a1+b1+j*t*mu, -b1, a1*gamma1, 0, 0;...
     -b2, -t^2+g/l2+a2+b2+b3+j*t*mu, a2*gamma1, 0, 0;...
     0, -b4, a3*gamma1, -b5, 0;...
     0, 0, a4*gamma1, -t^2+g/l4+a4+b6+b7+j*t*mu, -b7;...
     0, 0, a5*gamma1, -b8, -t^2+g/l5+a5+b8+j*t*mu];
amp3=simplify(det(D)/det(A));

% PENDULUM 4
E = [-t^2+g/l1+a1+b1+j*t*mu, -b1, 0, a1*gamma1, 0;...
     -b2, -t^2+g/l2+a2+b2+b3+j*t*mu, -b3, a2*gamma1, 0;...
```

```
91      0, -b4, -t^2+g/l3+a3+b4+b5+j*t*mu, a3*gamma1, 0;...
        0, 0, -b6, a4*gamma1, -b7;...
93      0, 0, 0, a5*gamma1, -t^2+g/l5+a5+b8+j*t*mu];
amp4=simplify(det(E)/det(A));
95
% PENDULUM 5
97 F = [-t^2+g/l1+a1+b1+j*t*mu, -b1, 0, 0, a1*gamma1;...
       -b2, -t^2+g/l2+a2+b2+b3+j*t*mu, -b3, 0, a2*gamma1;...
99      0, -b4, -t^2+g/l3+a3+b4+b5+j*t*mu, -b5, a3*gamma1;...
        0, 0, -b6, -t^2+g/l4+a4+b6+b7+j*t*mu, a4*gamma1;...
101     0, 0, 0, -b8, a5*gamma1];
amp5=simplify(det(F)/det(A));
103
figure('Name','Analytical measurement - tmp','NumberTitle','off')
105
% Plot the amplitudes verus the driving frequency
107 hold on
e1=ezplot(abs(amp1),[5, 15, 0, 4]);
109 setcurve('color','red')
e2=ezplot(abs(amp2),[5, 15, 0, 4]);
111 setcurve('color','blue')
e3=ezplot(abs(amp3),[5, 15, 0, 4]);
113 setcurve('color','green')
e4=ezplot(abs(amp4),[5, 15, 0, 4]);
115 setcurve('color','magenta')
e5=ezplot(abs(amp5),[5, 15, 0, 4]);
117 setcurve('color','black')
hold off
119
% Get the data so that we can save it
121 x1=get(e1,'xdata');
y1=get(e1,'ydata');
123 x2=get(e2,'xdata');
y2=get(e2,'ydata');
125 x3=get(e3,'xdata');
y3=get(e3,'ydata');
127 x4=get(e4,'xdata');
y4=get(e4,'ydata');
129 x5=get(e5,'xdata');
y5=get(e5,'ydata');
131
% Determine the resonance frequencies of this system
133 [ymax1 i1]=max(y1);
[ymax2 i2]=max(y2);
135 [ymax3 i3]=max(y3);
[ymax4 i4]=max(y4);
137 [ymax5 i5]=max(y5);

139 % And print them to the console
str = sprintf('Experimental:\n\tw1 = %f\n\tw2 = %f\n\tw3 = %f\n\tw4
      = %f\n\tw5 = %f', x1(i1), x1(i2), x1(i3), x1(i4),x1(i5));
141 disp(str)

143 % Now close the old plot
close(findobj('type','figure','name','Analytical measurement - tmp'
    ))
145
```

```
% And save the data
save('simulation_analytical.mat', 'x1', 'x2', 'x3', 'x4', 'x5', 'y1
    ', 'y2', 'y3', 'y4', 'y5')
clear all
close all
```

measurements_simulation_and_nonlinear_vs_linear.m

```
% In this section we run a simulation from w = 5 to w = 15 rad/s.
    We
% compare the result from this simulation with the analytical
    result in
% result_analytical_vs_simulation.m. We assume linearity, since the
% analytical result is linear as well.

% First, let's do some housekeeping
clear all
close all
clc

% Set frequency domain and resolution
omega_low = 5;
omega_high = 15;
N=2000;

% Do the actual measurement (linearity is assumed)
[x maxima]=solution_pulse_continuous_driving([omega_low omega_high
    ], N, true);
progressbar(1) % otherwise the progress bar will open as well

% Save data
save simulation_analytical_vs_simulation.mat
clear all
close all

%
    ------------------------------------------------------------------------

% In this section we are going to compare the effect of
    nonlinearity vs
% linearity.

% Set frequency domain and resolution
omega_low = 5;
omega_high = 15;
N=2000;

% Do the actual measurements
% Non-linear
[xnonlinear maximanonlinear]=solution_pulse_continuous_driving([
    omega_low omega_high], N, false);
progressbar(1) % otherwise the progress bar will open as well

% Linear
[xlinear maximalinear]=solution_pulse_continuous_driving([omega_low
     omega_high], N, true);
```

```
progressbar(1) % otherwise the progress bar will open as well

save simulation_nonlinear_vs_linear.mat
clear all
close all
```

solution_pulse_continuous_driving.m

```
function [x maxima]=solution_pulse_continuous_driving(
    frequency_domain, steps, linear)

% Transfer neccesary variables to pulse_continuous_driving.m by
    making them global
global g
global a_1
global a_2
global a_3
global a_4
global a_5
global b_1
global b_2
global b_3
global b_4
global b_5
global b_6
global b_7
global b_8
global l_1
global l_2
global l_3
global l_4
global l_5
global driving_amplitude
global mu
global omega
global linearity
linearity = linear;

% Define the masses of the pendula
m1 = .235;
m2 = .240;
m3 = .25;
m4 = .255;
m5 = .22;

% Axle-coupling spring constants
kappa_as_1 = 0.13;
kappa_as_2 = 0.12;
kappa_as_3 = 0.101;
kappa_as_4 = 0.112;
kappa_as_5 = 0.121;

% Pendula-coupling springs constants
kappa_over_1 = 0.012;
kappa_over_2 = 0.016;
kappa_over_3 = 0.010;
```

```
kappa_over_4 = 0.011;

% The pendula lengths
l_1 = 0.1;
l_2 = 0.15;
l_3 = 0.2;
l_4 = 0.25;
l_5 = 0.3;

% Defining other constants
g = 9.81;
mu = 0.1;
driving_amplitude = 0.1;

a_1 = kappa_as_1/(m1*l_1^2);
a_2 = kappa_as_2/(m2*l_2^2);
a_3 = kappa_as_3/(m3*l_3^2);
a_4 = kappa_as_4/(m4*l_4^2);
a_5 = kappa_as_5/(m5*l_5^2);
b_1 = kappa_over_1/(m1*l_1^2);
b_2 = kappa_over_1/(m2*l_2^2);
b_3 = kappa_over_2/(m2*l_2^2);
b_4 = kappa_over_2/(m3*l_3^2);
b_5 = kappa_over_3/(m3*l_3^2);
b_6 = kappa_over_3/(m4*l_4^2);
b_7 = kappa_over_4/(m4*l_4^2);
b_8 = kappa_over_4/(m5*l_5^2);

% Initial angles
theta1_0 = 0;
theta2_0 = 0;
theta3_0 = 0;
theta4_0 = 0;
theta5_0 = 0;

% Initial angular velocities
omega1_0 = 0;
omega2_0 = 0;
omega3_0 = 0;
omega4_0 = 0;
omega5_0 = 0;

% Start- and end time of the numerical integration
t_0 = 0;
t_end = 300;

% Creating an array, containing the initial conditions
theta_0 = [t_0 theta1_0 theta2_0 theta3_0 theta4_0 theta5_0
    omega1_0 omega2_0 omega3_0 omega4_0 omega5_0];

% Pre-define arrays to contain the maximum amplitudes of each
    pendulum at a
% specific driving frequency and also pre-define the x array that
    we return
% (which is actually omega)
maxima1 = [];
maxima2 = [];
```

```
maxima3 = [];
maxima4 = [];
maxima5 = [];
x = [];

% Keep track of which step we're at
indx=1;
progressbar;
for i=linspace(frequency_domain(1), frequency_domain(2), steps)
    indx = indx+1;

    % Set the current value for omega
    omega = i;

    % Append this value to our x array
    x = [x i];

    % Numerical integration by the ode45 function
    [T,theta]=ode45(@pulse_continuous_driving,[t_0 t_end],theta_0);

    % Figure out which element of the array corresponds to roughly
        the last
    % 50 seconds of data (ODE45 randomly chooses dt's)
    search_ind = length(find(T<250));

    % And finally, determine the maximum amplitude of the pendula
        at this
    % specific frequency and append it to yee big ol' array!
    maxima1=[maxima1 max(theta(search_ind:end,2))];
    maxima2=[maxima2 max(theta(search_ind:end,3))];
    maxima3=[maxima3 max(theta(search_ind:end,4))];
    maxima4=[maxima4 max(theta(search_ind:end,5))];
    maxima5=[maxima5 max(theta(search_ind:end,6))];

    % Update the progress bar to indicate that heavy machinery is
        at work
    progressbar(indx / steps);
end

% Finally, build a big ol' matrix o' loot! Har-har-har
maxima = cat(1,maxima1,maxima2,maxima3,maxima4,maxima5);
end
```

pulse_continuous_driving.m

```
function dtheta = pulse_continuous_driving(t,theta)

% Return value of constants defined in oplossing_pulse.m
global g
global a_1
global a_2
global a_3
global a_4
global a_5
global b_1
global b_2
```

```
global b_3
global b_4
global b_5
global b_6
global b_7
global b_8
global l_1
global l_2
global l_3
global l_4
global l_5
global driving_amplitude
global mu
global omega
global linearity

% The actual driving signal, this can be arbitrarily chosen. In this case,
% a cosine is chosen as the input.
f = @(t) driving_amplitude*cos(omega*t);

% The system of 5 second order differential equations has been rewritten as
% a system of 10 first order differential equations.
dtheta(1) = 1;                  % d/dt(t) = 1
dtheta(2) = theta(7);
dtheta(3) = theta(8);
dtheta(4) = theta(9);
dtheta(5) = theta(10);
dtheta(6) = theta(11);

% We consider two possible cases: linearity, or non-linearity
if linearity
    dtheta(7) = -(g/l_1)*(theta(2)) - a_1*(theta(2)-f(theta(1))) - b_1*(theta(2)-theta(3)) -mu*theta(7);
    dtheta(8) = -(g/l_2)*(theta(3)) - a_2*(theta(3)-f(theta(1))) - b_2*(theta(3)-theta(2)) - b_3*(theta(3)-theta(4)) - mu*theta(8);
    dtheta(9) = -(g/l_3)*(theta(4)) - a_3*(theta(4)-f(theta(1))) - b_4*(theta(4)-theta(3)) - b_5*(theta(4)-theta(5)) - mu*theta(9);
    dtheta(10) = -(g/l_4)*(theta(5)) - a_4*(theta(5)-f(theta(1))) - b_6*(theta(5)-theta(4)) - b_7*(theta(5)-theta(6)) - mu*theta(10);
    dtheta(11) = -(g/l_5)*(theta(6)) - a_5*(theta(6)-f(theta(1))) - b_8*(theta(6)-theta(5)) - mu*theta(11);
else
    dtheta(7) = -(g/l_1)*sin(theta(2)) - a_1*(theta(2)-f(theta(1))) - b_1*(theta(2)-theta(3)) -mu*theta(7);
    dtheta(8) = -(g/l_2)*sin(theta(3)) - a_2*(theta(3)-f(theta(1))) - b_2*(theta(3)-theta(2)) - b_3*(theta(3)-theta(4)) - mu*theta(8);
    dtheta(9) = -(g/l_3)*sin(theta(4)) - a_3*(theta(4)-f(theta(1))) - b_4*(theta(4)-theta(3)) - b_5*(theta(4)-theta(5)) - mu*theta(9);
    dtheta(10) = -(g/l_4)*sin(theta(5)) - a_4*(theta(5)-f(theta(1))) - b_6*(theta(5)-theta(4)) - b_7*(theta(5)-theta(6)) - mu*
```

```
        theta(10);
53      dtheta(11) = -(g/l_5)*sin(theta(6)) - a_5*(theta(6)-f(theta(1))
        ) - b_8*(theta(6)-theta(5)) - mu*theta(11);
end
55
dtheta = dtheta';
```

Appendix B

MATLAB Files Chapter 4

pendulum_inverse_fourier.m

```
function [t_signal,z_signal] = pendulum_inverse_fourier()

% Define constants
mu          = 12.3396;      % Offset frequency
sigma       = 2.5;          % Gaussian curve shaping factor
t_start     = -100;         % Starting time in time domain
t_end       = -t_start;     % End time is minus start time
alpha       = 1;            % Amplitude factor of the gaussian
    curve

% Sampling frequency
ws = 50*(mu + 4*sigma);
% Corresponding time step
dt = (2*pi)/ws;

% Number of datapoints
N = (t_start-t_end)/dt +1;
% Making the number of datapoints 2^k for some integer k
N = 2^nextpow2(N);

% defining the time array
t = linspace(t_start,t_end,N);
% New time-step as N changed
dt = t(2)-t(1);
% New sampling frequency
ws = 2*pi/dt;

% Frequency array which spans N/2 points up to frequency ws/2
omega       = linspace(0,ws/2,N/2);

% Function that describes the amplitude in frequency domain,
% scaled with T
amplitude   = 1/(2*-t_start)*alpha*sqrt(2*pi)/sigma*exp(-(omega-mu)
    .^2/(2*sigma^2));
```

```
% For inverse fourier transforms, we need to flip this
%amplitude spectrum at 0.5*ws
amplitude    = [amplitude(1:end) flipdim(amplitude(1:end),2)];

% We will now manually construct a phase spectrum
fase = ones(1,length(amplitude));
[a,b] = max(amplitude);

for n = 1:(b-1)
    fase(n) = 0;
end
for n = b:(length(amplitude)-b+1)
    fase(n) = 0;
end
for n = (length(amplitude)-b):length(amplitude)
    fase(n) = 0;
end

% Determine the actual frequency spectrum of our signal
complex_amplitude = amplitude.*exp(i*fase);

% Now we define our actual frequency array, which spans from
% 0 to ws
omega = linspace(0,ws,N);

% Plot our frequency amplitude spectrum
plot(omega,abs(complex_amplitude))
xlabel('Angular frequency (rad/s)')
ylabel('Amplitude (a.u.)')
title(['Amplitude spectrum [N=' num2str(N) ', \omega_s=' num2str(ws
    ) ', \mu=' num2str(mu) ', \sigma=' num2str(sigma) ']'])

% Time domain
% It's now time to determine the time signal that belongs
% to this frequency spectrum
Z = ifft(complex_amplitude)*N; % times N for scaling
z = ifftshift(Z);

% This is a comparison result, the unchanged signal
y_orig = alpha*exp(-t.^2*sigma^2/2).*(exp(i*mu*t)+exp(-i*mu*t));
envelope = 2*alpha*exp(-t.^2*sigma^2/2);

% Energy content of both signals
E1 = trapz(t,abs(y_orig).^2);
E2 = trapz(t,abs(z).^2);

% Plotting the result on time domain
figure
plot(t,abs(z).*cos(angle(z)),t,y_orig)
hold on
plot(t,envelope,'r')
plot(t,-envelope,'r')
hold off
xlabel('angular frequency (rad/s)')
ylabel('\gamma')
title('Real part of time signal')
xlim([-10 10]);
```

```
% The phase spectrum
figure
plot(omega,fase)
xlabel('Angular frequency (rad/s)')
ylabel('Phase (rad)')
title('Phase as function of angular frequency')
% The imaginary part (should be around zero)
figure
plot(t,abs(z).*sin(angle(z)))
xlabel('Time (s)')
ylabel('\gamma')
title('Imaginary part of time signal')

% The following part is to determine the cut off time
typical_width = sqrt(16/sigma^2);
integer = 0;

for n = (length(t)/2):length(t)
    if abs(t(n)-typical_width)<dt
        integer = n;
        if abs(t(n)-typical_width) > abs(t(n+1)-typical_width)
            integer = n + 1;
        end
    end
end

typical_frequency = mu;
solution_interval = (2*pi)/typical_frequency;
ratio = round(solution_interval/dt);

% Checking if ratio is an even number
if mod(ratio,2) == 0
    ratio = ratio;
else
    ratio = ratio+1;
end

intersect = 10^-2;
array = ones(1,length(z));

% Searching for a zero of \gamma_s (t)
for n = integer:(ratio/2+integer)
    if abs(real(z(n))) < intersect
        array(n) = abs(real(z(n)));
    end
end

[value,integer] = min(array);

% Define the signals on their new time domain

steps = round(typical_width/dt);

t_signal = [t((end-integer-2*steps):(integer+8*steps))];
t = [t((end-integer):integer)];
y_orig = [y_orig((end-integer):integer)];
envelope = [envelope((end-integer):integer)];
```

```
z_signal = [zeros(1,length(z(1:end-integer-1))) z((end-integer):
    integer) zeros(1,length(z(integer+1:end)))];
z_signal = [z_signal((end-integer-2*steps):(integer+8*steps))];
z = [z((end-integer):integer)];

% Plotting the signals on their new time domain
figure
plot(t_signal,real(z_signal))
xlabel('time(s)')
ylabel('\gamma_s')
title('Time signal on new time domain')

% Again determining their energy content
E1 = trapz(t,abs(y_orig).^2);
E2 = trapz(t,abs(real(z)).^2);
disp(E1)
disp(E2)

% Calculating the scale factor
scalefactor = sqrt(E1/E2);
z_signal = z_signal*scalefactor;

% Plotting the rescaled time signals
figure
plot(t,abs(z).*cos(angle(z))*scalefactor,t,y_orig);
hold on
plot(t,envelope,'r');
plot(t,-envelope,'r');
hold off
xlabel('time(s)')
ylabel('\gamma_s')
title('Rescaled time signal')
xlim([t(1) t(end)])

% Checking if they have the same energy content
E1 = trapz(t,abs(y_orig).^2);
E2 = trapz(t,abs(z*scalefactor).^2);
disp(E1)
disp(E2)

end
```

pulse.m

```
function dtheta = pulse(t,theta)

% Return value of constants defined in oplossing_pulse.m
global g
global a_1
global a_2
global a_3
global a_4
global a_5
global b_1
global b_2
global b_3
```

```
global b_4
global b_5
global b_6
global b_7
global b_8
global l_1
global l_2
global l_3
global l_4
global l_5
global driving_amplitude
global mu
global time_signal
global ifftZ

% The actual driving signal, calculated from the inverse Fourier transform,
% which is a discrete signal. Because ode45 calculates its own optimal time
% step, the points at which f(t) is defined will not match the
% corresponding time values of ode45. Therefore an interpolation of f(t) is
% calculated using a cubic spline interpolant.
f = @(t) driving_amplitude*csapi(time_signal,real(ifftZ),t);

% The system of 5 second order differential equations has been rewritten as
% a system of 10 first order differential equations.
dtheta(1) = 1;                                          % d/dt(t) = 1
dtheta(2) = theta(7);
dtheta(3) = theta(8);
dtheta(4) = theta(9);
dtheta(5) = theta(10);
dtheta(6) = theta(11);

dtheta(7) = -(g/l_1)*sin(theta(2)) - a_1*(theta(2)-f(theta(1))) - b_1*(theta(2)-theta(3)) -mu*theta(7);
dtheta(8) = -(g/l_2)*sin(theta(3)) - a_2*(theta(3)-f(theta(1))) - b_2*(theta(3)-theta(2)) - b_3*(theta(3)-theta(4)) - mu*theta(8);
dtheta(9) = -(g/l_3)*sin(theta(4)) - a_3*(theta(4)-f(theta(1))) - b_4*(theta(4)-theta(3)) - b_5*(theta(4)-theta(5)) - mu*theta(9);
dtheta(10) = -(g/l_4)*sin(theta(5)) - a_4*(theta(5)-f(theta(1))) - b_6*(theta(5)-theta(4)) - b_7*(theta(5)-theta(6)) - mu*theta(10);
dtheta(11) = -(g/l_5)*sin(theta(6)) - a_5*(theta(6)-f(theta(1))) - b_8*(theta(6)-theta(5)) - mu*theta(11);

dtheta = dtheta';
```

solution_pulse.m

```
function solution_pulse()

% First clean up everything
```

```
clear all
close all
clc

% Pendula masses
m = mean([0.235 0.240 0.25 0.255 0.22]);
m_1 = m;
m_2 = m;
m_3 = m;
m_4 = m;
m_5 = m;

kappa1 = mean([0.13 0.12 0.101]);
kappa2 = mean([0.012 0.016 0.010 0.011]);

% Axle-coupling spring constants
kappa_as_1 = kappa1;
kappa_as_2 = kappa1;
kappa_as_3 = kappa1;
kappa_as_4 = kappa1;
kappa_as_5 = kappa1;

% Pendula-coupling springs constants
kappa_over_1 = kappa2;
kappa_over_2 = kappa2;
kappa_over_3 = kappa2;
kappa_over_4 = kappa2;

% Transfer neccesary variables to pulse.m by making them global
global g
global a_1
global a_2
global a_3
global a_4
global a_5
global b_1
global b_2
global b_3
global b_4
global b_5
global b_6
global b_7
global b_8
global l_1
global l_2
global l_3
global l_4
global l_5
global driving_amplitude
global mu
global time_signal
global ifftZ

% Defining the constants
g = 9.81;

l_1 = 0.1;
```

```
l_2 = 0.2;
l_3 = 0.3;
l_4 = 0.4;
l_5 = 0.5;

a_1 = kappa_as_1/(m_1*l_1^2);
a_2 = kappa_as_2/(m_2*l_2^2);
a_3 = kappa_as_3/(m_3*l_3^2);
a_4 = kappa_as_4/(m_4*l_4^2);
a_5 = kappa_as_5/(m_5*l_5^2);

b_1 = kappa_over_1/(m_1*l_1^2);
b_2 = kappa_over_1/(m_2*l_2^2);
b_3 = kappa_over_2/(m_2*l_2^2);
b_4 = kappa_over_2/(m_3*l_3^2);
b_5 = kappa_over_3/(m_3*l_3^2);
b_6 = kappa_over_3/(m_4*l_4^2);
b_7 = kappa_over_4/(m_4*l_4^2);
b_8 = kappa_over_4/(m_5*l_5^2);

mu = 0.1;
driving_amplitude = 1;

% Initial angles
theta1_0 = 0;
theta2_0 = 0;
theta3_0 = 0;
theta4_0 = 0;
theta5_0 = 0;

% Initial angular velocities
omega1_0 = 0;
omega2_0 = 0;
omega3_0 = 0;
omega4_0 = 0;
omega5_0 = 0;

% Calculating the inverse fourier transform of the frequency domain
[time_signal,ifftZ] = pendulum_inverse_fourier;

% Start- and end time of the numerical integration
t_0 =  min(time_signal);
t_end = max(time_signal);

% Creating an array, containing the initial conditions
theta_0 = [t_0 theta1_0 theta2_0 theta3_0 theta4_0 theta5_0
    omega1_0 omega2_0 omega3_0 omega4_0 omega5_0];

% Numerical integration by the ode45 function
[T,theta]=ode45(@pulse,[t_0 t_end],theta_0);

% Plotting the numerical solutions
plot(T,theta(:,2),T,theta(:,3),T,theta(:,4),T,theta(:,5),T,theta
    (:,6));
legend('\theta_1','\theta_2','\theta_3','\theta_4','\theta_5');
xlabel('time (s)');
ylabel('amplitude (rad)')
```

```
116
% Plotting the numerical solutions in seperate figures
118 figure
subplot(3,2,1), plot(T,theta(:,2)), xlabel(''), ylabel(''), title('
    n=1');
120 subplot(3,2,2), plot(T,theta(:,3),'g'), xlabel(''), ylabel(''),
    title('n=2');
subplot(3,2,3), plot(T,theta(:,4),'r'), xlabel(''), ylabel('\theta(
    t)'), title('n=3');
122 subplot(3,2,4), plot(T,theta(:,5),'c'), xlabel('t(s)'), ylabel(''),
     title('n=4');
subplot(3,2,5), plot(T,theta(:,6),'m'), xlabel(''), ylabel(''),
    title('n=5');
124
end
```